https://ntrs.nasa.gov/search.jsp?R=19640014901 2020-03-24T06:26:47+00:00Z

NASA TECHNICAL NOTE

NASA TN D-2067

c.1

LOAN COPY: RE
AFWL (WLI
KIRTLAND AFB, N

TECH LIBRARY KAFB, NM
0154595

NASA TN D-2067

EFFECTS OF HIGH SUSTAINED ACCELERATION ON PILOTS' PERFORMANCE AND DYNAMIC RESPONSE

by Melvin Sadoff

Ames Research Center
Moffett Field, Calif.

RECEIVED
6 JUL 1964
Technical Library
AF Weapons
Laboratory

NATIONAL AERONAUTICS AND SPACE ADMINISTRATION • WASHINGTON, D. C. • JULY 1964

TECH LIBRARY KAFB, NM
0154595

EFFECTS OF HIGH SUSTAINED ACCELERATION ON PILOTS' PERFORMANCE AND DYNAMIC RESPONSE

By Melvin Sadoff

Ames Research Center
Moffett Field, Calif.

NATIONAL AERONAUTICS AND SPACE ADMINISTRATION

For sale by the Office of Technical Services, Department of Commerce,
Washington, D.C. 20230 -- Price $1.50

EFFECTS OF HIGH SUSTAINED ACCELERATION ON P.

PERFORMANCE AND DYNAMIC RESPONSE

By Melvin Sadoff

Ames Research Center
Moffett Field, Calif.

SUMMARY

A study was conducted by Ames Research Center on the human centrifuge at the U. S. Naval Air Development Center, Johnsville, Pa., to determine the effects of sustained high acceleration on pilot control capabilities. The results showed that the predominant effect of acceleration stress was an increased attenuation of the pilot's dynamic response and an associated large increase in his errors at the higher frequency components in the task command input function.

This impairment of the pilot's control capability suggests that it may not be desirable to impose precise attitude-stabilization tasks on human pilots when high-frequency control during periods of high sustained accelerations is required of him. Results of the present study indicate that for control frequencies above about 1/6 cps and at acceleration levels above about 6 g, an appreciable deterioration in pilot attitude-control performance is expected.

INTRODUCTION

In recent years, a systems approach to the design of advanced manned systems has been given considerable attention. In this approach, the pilot, vehicle, control-surface actuators, and other elements are regarded as a closed-loop feedback control system. This procedure has been used successfully for years in the design of automatic control systems; its extension to manned-system design is clearly desirable. Before this concept can be implemented for piloted vehicle systems, however, it is necessary to acquire a basic understanding of one element, the pilot, since his control capabilities and limitations constitute information which is essential for this type of analysis.

Considerable progress has been made recently in documenting pilot-response characteristics over a wide range of simulated control tasks (refs. 1 to 4). However, little is known about how a pilot's control capabilities and response characteristics vary with changes in environmental stress. Since one of the primary environmental stresses imposed on the pilot of advanced aircraft and space vehicles is a wide range of linear accelerations, a brief

exploratory study was directed, in part, toward determining pilot performance and response characteristics at high levels of acceleration.

As part of a general NASA program, experimental studies were conducted by the Ames Research Center on the Aviation Medical Acceleration Laboratory centrifuge, Naval Air Development Center, Johnsville, Pa., to measure effects of sustained high levels of acceleration on the performance and physiology of pilots. Some of the results of these studies are reported in references 5 to 10. The primary purpose of the present report is to provide some basic additional information on the effects of high-acceleration levels on pilot control-task performance and on pilot-response characteristics. These data were obtained by conventional power spectral analysis techniques, using a digital program to extract the basic correlation functions and spectra required to determine pilot performance and dynamic response.

The convention established in reference 5 has been retained to describe the direction of the applied acceleration force. The terms eyeballs in (EBI), eyeballs out (EBO), and eyeballs down (EBD) correspond, respectively, to the accelerations A_X, $-A_X$, and A_N referred to a conventional airplane body-axis coordinate system.

NOTATION

A_N acceleration factor, ratio of acceleration force to weight, positive when directed from seat to head

A_X acceleration factor, ratio of acceleration force to weight, positive when directed from back to chest

AR amplitude ratio

F_s pilot control force, lb

g acceleration of gravity, 1 g = 32.2 ft/sec^2

H closed-loop pilot describing function, in./deg

i task input, deg

K_c vehicle gain

K_p pilot d-c gain, in./deg

$\overline{n^2}$ mean-square uncorrelated pilot control output, in.^{2}

n_c total pilot remnant (assumed injected at pilot output), in.

n_c^* pilot remnant due to nonlinear control response or "noise" injection, in.

$R_{ii}(\tau)$	autocorrelation of input function, deg^2
$R_{\epsilon\epsilon}(\tau)$	autocorrelation of task error, deg^2
$R_{\delta\delta}(\tau)$	autocorrelation of pilot control output, $in.^2$
$R_{\theta\theta}(\tau)$	autocorrelation of vehicle output, deg^2
s	Laplace transform variable
T_L	pilot lead time constant, sec
T_I	pilot lag time constant, sec
T_θ	numerator constant in pitch transfer function, sec
t	time, sec
Y_c	vehicle pitch transfer function, deg/in.
Y_p	pilot describing function, in./deg
Y_{CL}	closed-loop, pilot-vehicle system function, deg/deg
δ	pilot controller deflection, in.
$\overline{\delta^2}$	mean-square pilot control output, $in.^2$
ϵ	tracking error, deg
$\overline{\epsilon^2}$	mean-square tracking error, deg^2
ζ	vehicle short-period damping ratio in pitch
θ	vehicle pitch angle, deg
ρ	linear correlation
$\overline{\rho_a{}^2}$	average linear coherence, $1 - \frac{\overline{n^2}}{\overline{\delta^2}}$
$\overline{\sigma^2}$	mean-square task input, deg^2
τ	autocorrelation function argument, sec
τ_p	pilot visual reaction time lag, sec
Φ_{ii}	task input power spectrum
$\Phi_{\epsilon\epsilon}$	tracking error power spectrum
$\Phi_{\delta\delta}$	pilot control output power spectrum

$\Phi_{\theta\theta}$	vehicle pitch angle power spectrum
Φ_{nn}	closed-loop remnant power spectrum
Φ_{nn_c}	open-loop remnant power spectrum
$\Phi_{i\epsilon}$	cross-power spectrum of task input and tracking error
$\Phi_{i\delta}$	cross-power spectrum of task input and pilot-control deflection
$\Phi_{i\theta}$	cross-power spectrum of task input and vehicle pitch angle
φ	phase angle, deg
ω	angular frequency, radians/sec
ω_c	pilot-vehicle system crossover frequency, radians/sec
ω_n	vehicle longitudinal short-period frequency, radians/sec

Subscripts

I	imaginary part of cross spectrum
R	real part of cross spectrum
r	attributed to pilot remnant

TEST EQUIPMENT AND PROCEDURE

Apparatus

The human centrifuge at the Aviation Medical Acceleration Laboratory, Naval Air Development Center, Johnsville, Pa., was used in this research program. A detailed description of this device is provided in references 11 and 12.

Since a pilot's tolerance and ability to perform a manual control function during sustained high-acceleration levels depend largely on the effectiveness of his restraint system, considerable effort was made to develop a system suitable for use in NASA's acceleration research program. The result was an interchangeable mobile pilot-restraint system described in detail in reference 13. A unique feature of this system is that it restrains the pilot during sustained high accelerations in the EBO as well as EBI directions.

The pilot controls used in this study were a finger-operated, two-axis side-arm controller, and toe pedals. Photographs and force-deflection

characteristics of the pilot controls are presented in figures 1 and 2, respectively. Pilot comments in reference 5 indicated a general preference for this controller among those evaluated during the reference study.

Task

The pilot's performance was measured during pitch-attitude tracking with the cathode-ray tube display in figure 3. The pilot's task was to track a target that moved in an apparently random fashion through the angles i. The target forcing function i was generated by the sum of four sinusoids with the amplitude-frequency characteristics shown in the table below.

	Sine wave component			
	1	2	3	4
Amplitude, mean square, deg^2	14.4	6.3	2.0	1.0
Frequency, radians/sec	.28	.74	1.15	1.60

One cm on the oscilloscope was made equivalent to four degrees of target motion. Though no target motion was programmed in azimuth ψ, azimuth tracking errors could develop as a result of inadvertent lateral control inputs causing heading perturbations relative to the original zero heading reference. The test pilots were instructed to minimize both the pitch tracking error ϵ, as well as the inadvertent heading error ψ, generated during the performance test runs (see fig. 3).

The simulated vehicle for this study was representative of a high-performance or entry-type aircraft. The aircraft equations of motion used described a system with five degrees of freedom, with the vehicle forward velocity assumed constant. The pertinent stability and control derivatives used are listed in table I. The longitudinal short-period frequency and damping ratio associated with the longitudinal derivatives in table I were 3.35 radians per second and 0.53, respectively. These values were shown in reference 5 to result in satisfactory longitudinal handling characteristics for entry vehicles even at moderate sustained accelerations of the order of 7 g.

Figure 4 is a block diagram of the pilot's primary pitch-attitude control task. It should be noted that the pilot's display (fig. 3) provided the pilot with target motion i and vehicle motion θ, in addition to the tracking error ϵ; however, pilots' comments indicated the error signal was the primary visual cue used in the performance of the task.

Tests

The tests for which results are presented herein were conducted with four experienced test pilots - two from Ames Research Center, one from the Air

Force, and one from Manned Spacecraft Center. Prior to data runs at the higher accelerations, the pilots were conditioned to the effects of sustained accelerations and were familiarized with the piloting task and the centrifuge. Generally, the pilots were not exposed to accelerations greater than 6 g during the period of familiarization. The pilots were then briefed in detail before they were exposed to the high-acceleration runs. They were instructed to perform the control task continuously from the beginning of the run, through the complete acceleration-profile time history, to the termination of the run. The high-acceleration portion of the run could be terminated by the pilot or by either the doctor or engineer who were continuously monitoring the physiological and performance records. The test runs could be terminated as a result of either of the following factors: marked reduction in control-task performance; marked increase in physical discomfort or physiological symptoms, such as loss of vision, disorientation or vertigo, sudden onset of chest pain, etc.

ANALYSIS

A typical time history of acceleration and associated control-task performance is presented in figure 5. The normalized task-performance error given was averaged over 20-second time intervals.[1] It will be noted that during the acceleration ramps up to maximum acceleration and down again, large increases in the normalized error occurred. It is believed these error excursions resulted primarily from the disorienting effects of the large roll and pitch centrifuge gimbal motions required to orient the g vector in the proper direction (EBI in the present example). To avoid the transient effects of the up-acceleration ramp on pilot performance and response, the 15- or 20-second interval following the ramp was not analyzed. In the present example, as shown in figure 5, 100 seconds of data were analyzed, starting at 100 seconds from the beginning of the test run. Table II summarizes the acceleration levels and directions and the analysis times for the data.

In order to analyze the results using conventional, relatively simple, power-spectral techniques, it was necessary to assume that the actual primary control task illustrated in figure 4 could be simplified to the compensatory system shown in figure 6. This was believed justified since the pilots indicated their primary visual stimulus was the task error ϵ.

A detailed description of power-spectral techniques, as applied to the problem of extracting human-operator tracking performance and dynamic response for compensatory systems, such as that illustrated in figure 6, is provided in reference 1. Therefore, this approach is only briefly outlined here.

---

[1]Since the static portions of the test runs were 60 seconds long, it was convenient to use nonoptimum time intervals of 20 seconds. The optimum interval is about 22.6 seconds, or 2π divided by the lowest forcing-function frequency. A small part of the observed normalized error variations with time is probably due to the use of a nonoptimum time interval.

The signals $i(t)$, $\epsilon(t)$, $\delta(t)$, and $\theta(t)$ (fig. 6) were all recorded on magnetic tape during the test runs; subsequently, they were converted to digital form (0.1-second intervals) and analyzed on an IBM 7090 computer. A Tukey Spectrum Estimation Program obtained from the IBM SHARE library (Nancy Clark, Convair, San Diego, 5 December, 1958) was used to obtain the autocorrelations, cross correlations, spectrum, co-spectrum, and quadrature spectrum of two simultaneous time series. In the present study three time-series pairs were analyzed: input and error, input and pilot control output, and input and vehicle output. In addition, the coherence ρ^2 at each frequency between the time series pair is provided, and the phase angle between the time series pair at each frequency is given.

A representative set of the spectral and cross-spectral results obtained is presented in figure 7. These data, together with the correlation functions at zero argument (mean squares) of the task input, task error, and pilot control output, are the basic information required to determine the pilot's performance and dynamic-response characteristics.

The spectrum estimates at each of the four input frequencies (fig. 7) were used to estimate both the vehicle and pilot transfer functions at these frequencies. For example, as demonstrated in reference 1:

$$Y_c = \frac{\Phi_{i\theta}}{\Phi_{i\delta}} \tag{1}$$

and

$$Y_p = \frac{\Phi_{i\delta}}{\Phi_{i\epsilon}} \tag{2}$$

Since the input spectrum and the vehicle transfer function are know, a simple check of the accuracy of the spectral estimates was provided by the comparisons shown in figure 8. The vehicle transfer-function amplitude and phase computed from the spectral estimates (eq. (1)) agree very well with the actual vehicle characteristics (see figs. 8(b) and 8(c)); the comparison between the computed and actual input spectra in figure 8(a) is, however, only fair. It is possible that the actual input spectra varied during the test program because of inadvertent gain changes on the input. It should be pointed out that despite the apparent scatter in estimated input spectra, the relative amplitudes (for any one set of data), normalized with respect to the lowest frequency amplitude, corresponded closely with those for the actual spectra.

In addition to the above information, it was possible to determine the closed-loop pilot response, the open- and closed-loop system transfer functions, and the mean-square task input and task error by means of the following relationships:

$$H = \frac{Y_p}{1 + Y_p Y_c} = \frac{\Phi_{i\delta}}{\Phi_{ii}} \tag{3}$$

$$Y_p Y_c = \frac{\Phi_{i\theta}}{\Phi_{i\epsilon}} \tag{4}$$

$$Y_{CL} = \frac{Y_p Y_c}{1 + Y_p Y_c} = \frac{\Phi_{i\theta}}{\Phi_{ii}} \tag{5}$$

$$\overline{\epsilon^2} = R_{\epsilon\epsilon}(0) \tag{6}$$

$$\overline{\sigma^2} = R_{ii}(0) \tag{7}$$

A particularly valuable piece of information provided by the analysis was the coherence ρ^2 between the time-series pair involving the forcing function input and the pilot's control output. It is apparent from the block diagram assumed in figure 6, that the pilot's output is comprised of two parts - a part due to a linear operation Y_p on the error, and that portion not linearly coherent with the input. The latter portion $n_c(t)$ is the open-loop pilot remnant. It can be shown (see ref. 1) that the pilot's control output, in spectral form, is given by,

$$\Phi_{\delta\delta} = \left| \frac{Y_p}{1 + Y_p Y_c} \right|^2 \Phi_{ii} + \left| \frac{1}{1 + Y_p Y_c} \right|^2 \Phi_{nn_c} \tag{8}$$

or

$$\Phi_{\delta\delta} = |H|^2 \Phi_{ii} + \Phi_{nn} \tag{9}$$

since

$$\Phi_{nn} = \Phi_{\delta\delta} - |H|^2 \Phi_{ii}$$

$$= \Phi_{\delta\delta} - \frac{|\Phi_{i\delta}|^2}{\Phi_{ii}^2} \Phi_{ii}$$

$$= \Phi_{\delta\delta} \left\{ 1 - \left[\frac{|\Phi_{i\delta}|^2}{\Phi_{ii}\Phi_{\delta\delta}} \right] \right\}$$

then

$$\Phi_{nn} = \Phi_{\delta\delta}(1 - \rho^2) \tag{10}$$

where

$$\rho^2 = \frac{|\Phi_{i\delta}|^2}{\Phi_{ii}\Phi_{\delta\delta}}$$

Equation (10) has meaning, then, only when $\Phi_{ii} \neq 0$, that is, at the forcing-function frequencies.

In addition to the discrete values of ρ^2 defined only for the forcing-function frequencies, average values of linear coherence $\overline{\rho_a^2}$, which include pilot remnant outside the forcing-function frequency range, as well as the discrete-frequency values, can also be defined. It can be shown that,

$$\overline{\rho_a^2} = 1 - \frac{\overline{n^2}}{\overline{\delta^2}} \tag{11}$$

where

$$\overline{n^2} = \overline{\delta^2} - 2\sum_{1}^{4} |H|^2 \Phi_{ii} \tag{12}$$

That portion of the pilot remnant outside the forcing-function frequency range is given by

$$\overline{n^{*2}} = \overline{n^2} - 2\sum_{1}^{4} \Phi_{\delta\delta}(1 - \rho^2) \tag{13}$$

It is apparent from equation (10) that if ρ^2 approaches 1, the remnant approaches zero, and the estimated linear operator H (or Y_p) alone provides an adequate representation of the pilot's control response at the forcing-function frequencies. If ρ^2 is appreciably less than about 0.90 the remnant is a relatively large part of the total control output and the quasi-linear operators Y_p and H alone become less meaningful indicators of the pilot's total control behavior.

RESULTS AND DISCUSSION

In the following main sections, the effects of high sustained linear accelerations on control-task performances, pilot dynamic response and pilot-vehicle system response measures will be shown. The primary results are presented in figures 9 through 26 and in table III. In the presentation of these results, curves are faired through the data to reflect trends suggested by the available data.

Control-Task Performance

Over-all task performance.- The over-all control-task performance was determined from time histories of tracking runs such as those shown in figure 9. These time histories illustrate the large adverse effects of sustained acceleration stress on pilot performance. The results for 7 g (EBD) (fig. 9(b)) show a large increase in task error ϵ and a significant increase in pilot control output δ, relative to results for the 1 g static portion of the run (fig. 9(a)). The error data in figure 9, as well as those for the other test runs were reduced, as described in the Analysis section to the over-all performance measure ϵ^2/σ^2, the mean-square tracking error, normalized with respect to the mean-square forcing function. Results were averaged over time

intervals ranging from 48 to 100 seconds (see table II). For the type of input forcing function used, analysis errors, due to variations in run lengths analyzed, were considered negligible. The resulting curves in figure 10 show the effects of acceleration vector magnitude on this performance measure for the four test pilot subjects. In general, control-task performance remains unchanged up to about 6 g. Above 6 g, task performance deteriorates at a varying rate, depending on the pilot subject and on the acceleration direction. For transverse EBO and EBI accelerations the performance of pilots A and B decreases uniformly at about the same rate; for pilot D (EBI accelerations), the performance reduction is more severe,[2] and for pilot C (EBD accelerations), task performance decreases almost to zero[3] at 7 g. The inter-pilot and intra-pilot task performance variability at 1 g shown in figure 10 is not considered unusual or excessive. The reverse trend in performance for pilot B shown by the limited data in figure 10(b) is of interest, though it is not considered typical.

The results of associated physiological measures on test pilots at high sustained accelerations (refs. 6 to 10) suggest that the deterioration in their performance may have been due to physiological stress. During high EBI accelerations, the pilots were unable to respirate properly. Results in reference 9 indicate that tidal volume is reduced to little more than pulmonary dead space; consequently, alveolar ventilation is seriously diminished, and the pilots may suffer from "acceleration hypoxia," not unlike normal environmental hypoxia. During EBO accelerations, results in references 9 and 10 show that while the pilot suffered no respiratory effects, they did experience tearing and blurred vision. At high EBD accelerations, the problem is mainly in the cardiovascular system, which attempts to maintain blood-flow rates at normal unstressed levels by means of an increase in heart rate. For accelerations above 6 g, this regulatory mechanism is unable to compensate; blood flow to the brain is diminished, and pilot C reported symptoms of partial blackout.

The average measure of control-task performance for transverse accelerations is compared in figure 11 with results from a previous study (ref. 5). The reference results are presented for two levels of pitch damping: well damped ($\zeta \approx 0.34$) and lightly damped ($\zeta \approx 0.02$). In an evaluation of entry-vehicle handling qualities (fig. 4 of ref. 5) the well-damped vehicle of the reference study, as well as the vehicle of the present investigation, was considered satisfactory, and the lightly damped vehicle was rated unacceptable at moderate transverse accelerations of about 7 g. It is apparent in figure 11 that the results of the present study (in particular, the performance trend with acceleration) agree well with the results for the well-damped vehicle of the reference study. This result is not unexpected, since the control tasks (i.e., vehicle dynamics and task input) were essentially the same in the two investigations. The results in figure 11 also indicate that as the difficulty of the control task is increased (e.g., by reducing vehicle damping), the onset of a marked deterioration in performance occurs at lower accelerations.

[2]The performance deterioration during the high-g portion of this run may have been exaggerated by the pilots attention being diverted from the control task during extended communication with the medical monitor.

[3]Task performance approaches zero as the mean-square error approaches the mean-square input, that is, $\overline{\epsilon^2}/\overline{\sigma^2} = 1.0$.

Component-task performance.- In order to illustrate how the decrement in over-all task performance due to acceleration stress was distributed over the range of forcing-function frequencies, the error spectra $\Phi_{\epsilon\epsilon}$, normalized with respect to the input spectra Φ_{ii}, are plotted in figure 12 for the four task input frequencies. Results are presented for the 1 g EBD static runs and for the maximum acceleration levels experienced by each of the four test pilot subjects. These results are very illuminating since they indicate, in general, that a major part of the deterioration in over-all task performance resulted from the pilot's inability to track the higher frequency, lower amplitude components of the task input. For the lowest frequency sine wave (period of about 22 sec), results for three of the four pilots (pilots A, B, C) show very little effect of acceleration stress on component task error. It is apparent even for pilot C, who reported he was partially blacked-out during the 7 g EBD acceleration portion of the run, that he was still able to track the lowest frequency component of the input with practically no decrease in performance (fig. 12(c)).

Though the results in figure 12 show a moderate increase in normalized component-task error with frequency even for the unstressed condition, it is not clear why the adverse effects of acceleration stress on component-task performance are confined primarily to the higher frequencies. This may be due to the direct effects of physiological stress, that is, the pilots may not be able to discern the higher frequency, lower amplitude input commands. (This is a probable explanation for the observed results in fig. 12(c).) Other possible contributing factors are reduced manual dexterity, and reduced pilot motivation due to stress-induced physical discomfort.

Pilot Dynamic Response

In order to provide some basic information on the effect of acceleration stress on the pilot controller element of the system considered in this study, selected Bode plots of pilot dynamic response were prepared and are presented in figures 13 to 16. Pilot amplitude ratio and phase lag at 1 g and at the maximum g experienced by each of the four test pilots are shown as a function of task input frequency. Also provided are linear correlations ρ^2 which are a measure of how well the estimated transfer function, that is, amplitude and phase characteristics, represents the pilot at the forcing-function frequencies.

In figure 17(a) the average linear coherence $\overline{\rho_a{}^2}$ (eq. (11)) is plotted as a function of acceleration. Also provided in figure 17(b) is the pilot control output signal-to-noise ratio where

$$\frac{S}{N} = \frac{\overline{\rho_a{}^2}}{1 - \overline{\rho_a{}^2}}$$

These data, together with the linear describing function data and discrete-frequency values of ρ^2 (figs. 13 to 16), provide a complete description of the effects of sustained acceleration stress on pilot dynamic response. The

pilot dynamic-response results in figures 13 to 17 indicate that the primary effects of high sustained acceleration were: (a) a general reduction in pilot amplitude ratio (with a significant reduction in open-loop crossover frequency, ω_c), (b) increased pilot phase lag, and (c) significant reductions in ρ^2 and $\overline{\rho_a^2}$. These effects were particularly evident for pilots B, C, and D (figs. 14 to 16); in general, the pilot amplitude-ratio and phase characteristics suggest increased filtering or attenuation of the pilots' response to the higher frequency components of the forcing function. This is illustrated more clearly by the results shown in the table below where the transfer-function approximations associated with the results in figures 13 to 16 are given. (It should be noted that these approximations represent the simplest transfer-function form that could be used to give a reasonable fit to the limited data. With this assumed form, a best fit of the data provided in figs. 13 to 16 was obtained by appropriate adjustment of the pilot equalization (lag-lead) gain and reaction-time terms.)

Pilot	Acceleration environment	Fitted transfer function
A	1 g, static	$Y_p = 0.18\, e^{-0.4s}(1 + s)/(1 + 5s)$
	10 g, EBO	$Y_p = 0.10\, e^{-0.5s}(1 + s)/(1 + 3s)$
B	1 g, static	$Y_p = 0.04\, e^{-0.1s}(1 + 0.2s)/(1 + 1.4s)$
	14 g, EBI	$Y_p = 0.04\, e^{-0.3s}(1 + 0.65s)/(1 + 3s)$
C	1 g, static	$Y_p = 0.05\, e^{-0.2s}(1 + 0.5s)/(1 + 1.7s)$
	7 g, EBD	$Y_p = 0.13\, e^{-0.3s}(1 + s)/(1 + 10s)$
D	1 g, static	$Y_p = 0.065\, e^{-0.2s}(1 + 0.5s)/(1 + 1.7s)$
	8 g, EBI	$Y_p = 0.16\, e^{-0.3s}(1 + s)/(1 + 10s)$

It is evident from these results that acceleration stress mainly increased lag T_I in the pilots' response. This impairment in pilot response is reflected by both the appreciable decrease in total task performance and by the large deterioration in component-task performance shown in figures 10 and 12 for these three pilots. These results may also explain the decreased acceptance by the pilots of the higher frequency, lightly damped vehicle motions observed in connection with the handling qualities evaluation shown in figure 4 of reference 5.

The results for pilot A (fig. 13) indicate that the sustained 10 g EBO acceleration had relatively little effect on his dynamic-response characteristics. A small, uniform reduction in amplitude ratio is indicated, and very little change is apparent in either pilot phase lag or the linear correlation squared. As was noted previously (figs. 10(a) and 12(a)), very little effect

of acceleration on control-task performance was observed for this pilot. (It should not be inferred from these limited results that EBO accelerations are more advantageous from a task-performance standpoint than EBI accelerations. Results in references 14 and 15 show about the same deterioration in tracking performance for similar levels of EBI or EBO accelerations stress.)

Although most of the increase in task error with acceleration was generally attributable to changes in the pilots' describing function Y_p, a small part of the increase was due to an increase in pilot remnant. The portion of the component-task error spectra $\Phi_{\epsilon\epsilon}$ contributed by this factor is:

$$(\Phi_{\epsilon\epsilon})_r = |Y_c|^2 \Phi_{nn} \tag{14}$$

where Y_c is the vehicle transfer function and Φ_{nn} is the closed-loop remnant spectra. Since significant decreases in the linear coherence ρ^2 occurred only at the higher frequencies (figs. 14(c) and 15(c)), the increase in over-all task error was relatively small because the major portion of the total error was contributed by the component-task errors at the two lowest input frequencies. (See table III.) Though of minor consequence in terms of over-all control-task performance, the observed decrease in linear correlation is believed to be indicative of an important change in pilot-control behavior related to the imposed acceleration stress. These changes, together with the observed changes in the linear portion of the pilots' control-response behavior, may be due to the effects of physiological stress described in the preceding section. Another possibility is that the pilots' ability to establish an appropriate standard of task performance under the stress of high sustained accelerations may be impaired. Results in a NASA sponsored study (ref. 15) suggest this latter effect may be an important factor. The study showed that under moderate EBI or EBO acceleration stress of 6 g, the pilots reported, subjectively, they were performing the assigned control task better than at the reference static (1 g) condition; actual control-task measures, however, indicated that their performance had degraded appreciably. It was also shown that if the pilots were provided quantitative information on how well they had been performing (by means of an additional element in the pilots' display), their performance virtually ceased to deteriorate with acceleration.

Since it was observed that the coherence ρ^2 and the remnant Φ_{nn} are important factors describing pilot control response, a brief discussion of possible sources of the remnant is desirable. In reference 1 four major sources of the remnant term are postulated, that is, (a) pilot responses to inputs other than the system forcing function, (b) nonlinear pilot response to the system forcing function, (c) injection of "noise" by the pilot, which is unexplained by either linear or nonlinear correlation with the input commands, and (d) nonsteady, or time-varying, pilot response. Of these, it is felt that only source (a) could be ruled out because the only other inputs the pilots were likely to respond to were acceleration perturbations which were only a small part (±0.5 g) of the total acceleration stress imposed on the pilots. Furthermore, since the remnant increased appreciably only at the higher frequencies where the vehicle gain was relatively low, it is doubtful that the small acceleration perturbations due to control response at these frequencies would be an important source of information to the pilots. The nature of the

available remnant measures ρ^2 and $\overline{\rho_a^2}$ is such that, for the special forcing function used in the present study (four nonharmonically related sinusoids), decreases in ρ^2 would suggest source (d), time-varying pilot response, as an important remnant factor; whereas, significant decreases in $\overline{\rho_a^2}$ would indicate that remnant sources (b), (c) and (d) were all possible contributing factors. Since the results in figures 13 to 16 show significant decreases in ρ^2 (corresponding to 30 to 50 percent of the total pilot remnant), it is very likely that time-varying pilot response at high sustained accelerations was an important remnant source. The remaining remnant of about 50 to 70 percent of the total (determined from eq. (13)) is attributable to sources (b) and (c). Both of these sources, nonlinear pilot response and "noisy" control behavior by the pilots, are believed equally important remnant sources; however, this assumption cannot be established conclusively from the results of the present study.

Pilot-Vehicle System Response

In order to illustrate more clearly the effects of changes in the pilots' response measures on changes in open- and closed-loop system response measures, the results in figures 18 to 25 are provided. The open- and closed-loop system amplitude and phase for the reference static and high-acceleration portions of the selected test runs are plotted for the four test pilots.

Several interesting observations can be made with regard to the open-loop response characteristics shown in figures 18 to 21. Of particular interest is the fact that the open-loop transfer functions can be approximately represented over the range of forcing-function frequencies simply by a gain and an integral lag; that is

$$Y_p Y_c \approx \frac{K}{S}$$

This suggests that the pilots' control strategy was to adopt an equalization such that, over the range of input frequencies, the effects of the dominant time constants in the vehicle transfer function Y_c were suppressed. Since

$$Y_c = \frac{13.4(1 + 2.3s)}{s[(s^2/11.25) + (3.55s/11.25) + 1]} \tag{15}$$

then

$$Y_p \approx \frac{K_p e^{-\tau_p s}(1 + T_L s)}{(1 + T_I s)} \tag{16}$$

where $T_I \approx 2.3$ seconds and sufficient lead, T_L was inserted to counteract the phase lag introduced by his own reaction time delay τ_p, as well as that due to the second-order denominator term in the vehicle transfer function. Results for the pilots' open-loop response Y_p from the table in the preceding section show that the pilots did adapt roughly as suggested. For the

unstressed (1 g static runs), values of T_I ranged from 1.4 to 5 seconds with an average value of 2.4 seconds, and values of T_L varied from 0.2 to 1.0 second with an average of 0.5 second. For the high-g portions of these runs, T_I varied from 3 to 10 seconds (average of 6.5 sec), and T_L ranged from 0.6 to 1.0 second (average value, 0.9 sec).

Another observation that may be made from the open-loop results in figures 18 to 21 is that the open-loop crossover frequency ω_c invariably decreased with increase in acceleration stress. This is clearly demonstrated in figure 26 where the open-loop crossover frequency is plotted as a function of acceleration for each of the four test pilots. The open-loop crossover is a particularly informative piece of information since its inverse is roughly the dominant time constant of the closed-loop pilot-vehicle system and, as demonstrated in reference 16, ω_c is intimately related to the system mean-square error. Since the results indicated the pilots adapted their response so that the open-loop response appeared to be represented by a gain ($K \approx K_c K_p$) and an integral lag, the closed-loop system response is given approximately by

$$Y_{CL} = \frac{\theta}{i} \approx \frac{1}{(1/K_p K_c)s + 1} \tag{17}$$

where $K_p K_c$ is the open-loop crossover. A check of the actual closed-loop system-response characteristics (figs. 22 to 25) shows the above approximation for the closed-loop response is fairly good, particularly for the unstressed, 1 g results.

Implications of Results

In the preceding sections, it was observed that the dominant effects of high sustained acceleration stress on pilot response were increased filtering, or attenuating, at the higher frequencies, and increased short-time variability, as demonstrated by the decrease in linear coherence ρ^2. The former effect resulted in a significant decrease in the pilot-vehicle system crossover frequency and, consequently, in closed-loop system performance. This reduction in the pilots' ability to cope with the higher frequency components of the command input suggests that pilots should not be expected to control moderate-frequency commands, or lightly damped, moderate-frequency, vehicle motions at high sustained accelerations. More specifically, it might be expected from the present results that the pilots' ability to control lightly damped reentry vehicle motions will be impaired at acceleration levels above about 6 g for frequencies much greater than 1 or 2 radians per second. Also, the pilots should not be expected to cope with or control precisely, rigid-body or structural-mode attitude motions of launch vehicles for which boost accelerations and vehicle motions greater than about 6 g and 2 radians per second, respectively, are expected.

CONCLUSIONS

A centrifuge study was conducted to assess the effects of a sustained high acceleration on pilot control-task performance and dynamic-response characteristics for an attitude-stabilization task. Some general observations based on the results of this study are as follows:

1. Comparison of control-task performance measures for the 1 g reference condition and for sustained high acceleration indicated:

   a. Over-all task performance diminished rapidly at accelerations above 6 g.

   b. Control-task performance decrement for the lowest frequency component of the input function was fairly small but performance generally decreased to near zero levels for the higher frequency components.

2. The primary effects of high sustained accelerations on pilot dynamic-response measures were:

   a. Increased filtering or attenuation of pilot control response to the higher frequency input commands.

   b. Increased variability in pilot control response (or decreased coherence between control response and input commands), particularly for the higher frequency components of the input function.

3. Open-loop pilot-vehicle system response measures indicated:

   a. The pilots' control strategy was to adapt their response such that the open-loop system response was approximately a gain and an integral lag over the range of input command frequencies. This was particularly evident for the unstressed 1 g reference results.

   b. As a direct consequence of increased filtering in the pilots' response, the open-loop system crossover frequency decreased appreciably at high-acceleration environments. The associated increase in the dominant time constants of the closed-loop pilot-vehicle system was primarily responsible for the observed decrease in over-all and component-task performance.

Ames Research Center
National Aeronautics and Space Administration
Moffett Field, Calif., April 7, 1964

REFERENCES

1. McRuer, Duane T., and Krendel, Ezra S.: Dynamic Response of Human Operators. WADC Tech. Rep. 56-524, Oct. 1957.

2. Hall, I. A. M.: Effect of Controlled Element on the Human Pilot. WADC Tech. Rep. 57-509, 1958.

3. Elkind, Jerome I., Starr, Edward A., Green, David M., and Darby, Lucille D.: Evaluation of a Technique for Determining Time-Invariant and Time-Variant Dynamic Characteristics of Human Pilots. NASA TN D-1897, 1963.

4. Sadoff, Melvin, McFadden, Norman M., and Heinle, Donovan R.: A Study of Longitudinal Control Problems at Low and Negative Damping and Stability With Emphasis on Effects of Motion Cues. NASA TN D-348, 1961.

5. Creer, Brent Y., Smedal, Harald A., and Wingrove, Rodney C.: Centrifuge Study of Pilot Tolerance to Acceleration and the Effects of Acceleration on Pilot Performance. NASA TN D-337, 1960.

6. Smedal, Harald A., Creer, Brent Y., and Wingrove, Rodney C.: Physiological Effects of Acceleration Observed During a Centrifuge Study of Pilot Performance. NASA TN D-345, 1960.

7. Rogers, T. A., and Smedal, Harald A.: The Ventilatory Advantage of Backward Transverse Acceleration. Aerospace Medicine, vol. 32, Aug. 1961, pp. 737-40.

8. Holden, George R., Smith, Joseph R., Jr., and Smedal, Harald A.: Physiological Instrumentation Systems for Monitoring Pilot Response to Stress at Zero and High G. Aerospace Medicine, vol. 33, April 1962, pp. 420-7.

9. Smedal, Harald A., Rogers, T. A., and Duane, T. D.: Some Physiological Factors Affecting the Pilot Under High Sustained Accelerations. Paper presented at 33rd Annual Meeting of Aerospace Medical Association, Atlantic City, N. J., April 1962.

10. Creer, Brent Y., Stewart, John D., and Douvillier, Joseph G., Jr.: Influence of Sustained Accelerations on Certain Pilot-Performance Capabilities. Paper presented at 33rd Annual Meeting of Aerospace Medical Association, Atlantic City, N. J., April 1962.

11. Brooks, Charles E.: Data Sensing and Recording Techniques Established for the Human Centrifuge. NADC - MA-5306, U. S. Naval Air Development Center, Johnsville, Pa., 1954.

12. Crosbie, Richard J.: Cam Designing for the Human Centrifuge. NADC - MA-5512, Aviation Medical Acceleration Lab., U. S. Naval Air Development Center, Johnsville, Pa., 1955.

13. Vykukal, Hubert C., Gallant, Richard P., and Stinnett, Glen W.: An Interchangeable Mobile Pilot-Restraint System, Designed for Use in High Sustained Acceleration Force Fields. Aerospace Medicine, vol. 33, March 1962, pp. 279-85.

14. Creer, Brent Y., Smedal, Harald A., and Stewart, John D.: A Summary of the Influence of Sustained Acceleration on Pilot Performance and Pilot Physiology. Paper presented at Aerospace Medical Panel Meeting, Advisory Group for Aeronautical Research and Development, NATO, Paris, France, July 6-10, 1962.

15. Summers, L. G.: Human Tracking Performance Under Transverse Accelerations. Douglas Aircraft Company, Inc. Rep. LB 31116, Sept. 1962. (Prepared for NASA under Contract No. NASr-68.)

16. McRuer, Duane, and Graham, Dunstan: Pilot-Vehicle Control System Analysis. AIAA paper 63-310, Cambridge, Mass.

TABLE I.- AERODYNAMIC STABILITY DERIVATIVES

Derivative	Value	Units
L_p	-3.0	1/sec
L_β	-6.13	$1/sec^2$
N_r	-2.13	1/sec
N_β	9.86	$1/sec^2$
M_q	-3.11	1/sec
M_α	-9.86	$1/sec^2$
$M_{\delta_e}(\delta_e)_{max}$	-6.0	$1/sec^2$
$N_{\delta_r}(\delta_r)_{max}$	-2.0	$1/sec^2$
$L_{\delta_a}(\delta_a)_{max}$	-3.0	$1/sec^2$
$N_{\delta_a}(\delta_a)_{max}$	1.2	$1/sec^2$
Y_β	-.11	1/sec
N_α	-.44	1/sec

TABLE II.- ACCELERATION MAGNITUDES AND DIRECTIONS FOR DATA RUNS ANALYZED

Acceleration* level, g	Direction	Pilot	Pilot base	Analysis time, sec
10	Eyeballs out	A	Ames	57
10	Eyeballs in	B	Ames	68
10	Eyeballs in	B	Ames	67
14	Eyeballs in	B	Ames	100
7	Eyeballs down	C	Air Force	48
6	Eyeballs in	D	Manned Spacecraft Center	67
8	Eyeballs in	D		67

*1-minute static runs (1 g eyeballs down) were also analyzed to provide baseline measures for each of these high g runs.

TABLE III.- BASIC SPECTRA AND TRANSFER-FUNCTION DATA

A, g	ω	Φ_{ii}	$\Phi_{\epsilon\epsilon}$	$\Phi_{\delta\delta}$	$\Phi_{\theta\theta}$	$\Phi_{i\theta}$ AR	$\Phi_{i\theta}$ φ	$\Phi_{i\delta}$ AR	$\Phi_{i\delta}$ φ	$\Phi_{i\epsilon}$ AR	$\Phi_{i\epsilon}$ φ	Y_p AR	Y_p φ	Y_c AR	Y_c φ	Y_pY_c AR	Y_pY_c φ	H AR	H φ	Y_{CL} AR	Y_{CL} φ	ρ^2	$\overline{\rho_a^2}$
Pilot A																							
	0.28	574	43.1	0.178	680	621	-11.6	10.9	57.6	131	106	0.083	-48.4	57.0	-69.2	4.75	-118	0.019	57.6	1.09	-11.6	0.98	
1, EBD	.74	260	47.6	.177	237	253	-25.0	6.7	21.7	120	72	.056	-49.9	37.6	-46.7	2.10	-97	.026	21.7	.95	-25.0	.99	0.85
	1.15	60	11.0	.048	59	58	-23.5	1.6	23.7	24	77	.067	-52.9	36.2	-47.1	2.44	-100	.027	23.7	.99	-23.5	.96	
	1.60	33	14.4	.030	42	35	-36.2	1.0	13.2	22	76	.046	-63.1	35.9	-49.4	1.64	-113	.029	13.2	1.05	-36.2	.99	
	.28	580	59.3	.186	569	572	-17.5	10.6	43.6	176	78	.061	-34.9	53.9	-61.0	3.26	-96	.018	43.6	.98	-17.5	1.00	
10, EBD	.74	270	69.3	.177	240	252	-29.0	7.0	14.7	133	67	.053	-52.2	35.8	-43.7	1.90	-96	.026	14.7	.92	-29.0	1.00	.80
	1.15	65	20.3	.066	70	68	-28.1	1.8	15.7	31	76	.060	-60.7	36.8	-43.8	2.20	-104	.028	15.7	1.01	-26.4	.88	
	1.60	45	30.0	.042	45	43	-45.9	1.4	-3.3	35	66	.040	-68.9	30.8	-42.7	1.23	-112	.031	-3.3	.97	-47.2	.97	
Pilot B																							
	.28	746	63	.149	598	665	-15.6	10.6	44.8	208	59.5	.051	-14.7	62.9	-60.4	3.20	-75	.014	44.8	.89	-15.6	1.00	
1, EBD	.74	340	129	.171	194	253	-37.5	7.6	8.1	205	48.8	.037	-40.7	33.4	-45.6	1.23	-86	.022	8.1	.75	-37.5	1.00	.85
	1.15	83	47	.037	38	51	-52.5	1.7	-15.0	61	42.0	.027	-57.0	30.8	-37.4	.84	-94	.020	-15.0	.67	-52.5	.99	
	1.60	53	37	.013	12	21	-57.5	.8	-5.9	42	27.2	.018	-33.1	27.8	-51.6	.51	-85	.014	-5.9	.44	-57.5	.87	
	.28	737	259	.188	344	491	-33.2	11.4	20.6	423	39.5	.028	-18.9	42.9	-53.8	1.16	-73	.016	20.6	.67	-33.2	.94	
10, EBI	.74	339	385	.060	68	131	-84.9	4.3	-45.9	351	21.2	.013	-67.1	30.3	-39.0	.37	-106	.013	-45.9	.38	-84.9	.90	.83
	1.15	108	128	.022	26	50	-82.0	1.5	-54.7	114	24.6	.013	-79.2	34.3	-27.4	.44	-107	.014	-54.7	.45	-82.0	.98	
	1.60	44	60	.010	12	18	-85.2	.5	-37.9	52	19.1	.009	-57.0	39.6	-47.4	.35	-104	.010	-37.9	.36	-85.2	.49	
	.28	744	140	.139	540	624	-23.7	10.1	39.1	304	55.6	.033	-16.5	61.9	-62.7	2.05	-79	.014	39.1	.84	-23.7	.99	
1, EBD	.74	330	117	.146	188	246	-35.3	6.9	12.5	192	47.0	.036	-34.6	35.5	-47.7	1.28	-82	.021	12.5	.74	-35.3	.98	.88
	1.15	52	42	.016	22	41	-43.5	1.0	-11.6	54	31.3	.018	-42.9	42.7	-31.9	.76	-75	.019	-11.6	.55	-43.5	.89	
	1.60	52	61	.032	41	42	-65.4	1.3	-14.8	51	45.5	.025	-60.3	32.7	-50.6	.82	-111	.025	-14.8	.79	-65.4	.94	
	.28	719	197	.189	568	602	-25.0	11.0	38.8	308	55.7	.036	-17.0	54.6	-63.8	1.95	-81	.015	38.8	.84	-25.0	.89	
10, EBI	.74	324	312	.048	58	110	-75.2	3.4	-32.0	310	20.3	.011	-52.3	32.3	-43.2	.35	-95	.010	-32.0	.34	-75.2	.79	.69
	1.15	118	132	.038	43	52	-81.1	1.7	-37.9	116	27.2	.015	-65.1	30.2	-43.2	.45	-108	.014	-37.9	.47	-81.1	.70	
	1.60	56	68	.025	26	28	-80.9	1.0	-37.6	51	30.6	.020	-68.1	27.4	-43.3	.55	-111	.018	-37.6	.58	-80.9	.80	
	.28	805	98	.159	630	703	-18.9	11.1	47.7	263	58.6	.042	-10.8	63.0	-66.6	2.68	-77	.014	47.7	.88	-18.9	.99	
1, EBD	.74	355	198	.155	198	262	-46.9	7.5	-1.2	263	46.9	.028	-48.1	35.1	-45.6	.99	-94	.021	-1.2	.73	-46.9	.98	.89
	1.15	90	63	.028	35	52	-54.5	1.5	-16.6	73	36.8	.020	-53.4	34.3	-37.9	.70	-91	.017	-16.6	.58	-54.5	.97	
	1.60	65	52	.017	16	30	-66.4	1.0	-19.5	55	33.1	.018	-52.6	30.4	-46.9	.55	-100	.015	-19.5	.52	-66.4	.95	
	.28	825	109	.165	678	732	-18.2	10.6	31.9	263	60.4	.040	-28.5	69.0	-50.0	2.78	-79	.013	31.9	.89	-18.2	.82	
14, EBI	.74	370	329	.082	122	190	-64.8	4.8	-18.1	341	30.6	.014	-48.7	39.3	-46.7	.56	-95	.013	-18.1	.51	-64.8	.73	.62
	1.15	112	129	.035	34	39	-79.6	1.6	-46.3	103	23.3	.015	-69.6	24.3	-33.3	.37	-103	.014	-46.3	.38	-79.6	.66	
	1.60	63	60	.013	20	26	-69.4	.8	-23.2	54	25.6	.014	-48.8	33.7	-46.2	.47	-95	.012	-23.2	.44	-69.4	.56	
Pilot C																							
	.28	571	82	.143	550	555	-20.5	8.8	44.4	201	75.3	.044	-30.1	63.4	-64.9	2.77	-95	.015	44.4	.97	-20.5	.94	
1, EBD	.74	250	106	.121	148	192	-39.7	5.4	8.2	160	48.2	.034	-40.0	35.4	-47.9	1.20	-88	.022	8.2	.76	-39.7	.98	.86
	1.15	69	40	.028	33	46	-45.9	1.3	-3.5	47	43.3	.028	-46.7	34.6	-42.4	.98	-89	.019	-3.5	.70	-45.9	.94	
	1.60	34	19	.010	11	18	-47.3	.6	.6	24	35.0	.024	-34.5	30.8	-47.8	.72	-82	.017	.6	.55	-47.3	1.04	
	.28	567	150	.271	886	711	-23	12.0	40.3	280	109	.043	-68.6	59.3	-63.2	2.54	-132	.021	40.3	1.26	-23	.94	
7, EBD	.74	205	406	.132	145	159	-103	4.8	-45.7	289	32	.016	-77.9	33.4	-57.1	.56	-135	.023	-45.7	.76	-103	.80	.68
	1.15	115	93	.027	28	41	-52	1.4	-30.9	103	18	.014	-49.3	29.0	-21.1	.39	-70	.012	-30.9	.33	-52	.60	
	1.60	38	42	.021	36	26	-44	.6	-9.0	26	40	.024	-49.4	43.2	-34.5	1.05	-84	.017	-9.0	.69	-44	.30	
Pilot D																							
	.28	720	35	.213	618	663	-11.2	12.3	51.3	145	62.3	.085	-10.9	53.9	-62.5	4.57	-73	.017	51.3	.92	-11.2	.99	
1, EBD	.74	315	70	.204	255	276	-26.9	7.8	15.5	139	63.0	.056	-47.4	35.2	-42.4	1.98	-90	.025	15.5	.80	-26.9	.96	.77
	1.15	90	25	.048	50	67	-30.3	2.0	7.3	42	50.8	.047	-43.4	33.9	-37.6	1.58	-81	.022	7.3	.69	-30.3	.95	
	1.60	50	34	.035	33	33	-52.4	1.2	-5.0	35	49.7	.033	-54.6	28.4	-47.5	.94	-102	.023	-5.0	.46	-52.4	.94	
	.28	703	34	.242	699	696	-10.9	12.8	54.6	134	81.8	.096	-27.2	54.3	-65.5	5.21	-93	.018	54.6	.99	-10.9	.95	
6, EBI	.74	325	90	.212	260	289	-30.7	8.2	11.8	168	62.0	.049	-50.2	35.0	-42.5	1.72	-93	.025	11.8	.76	-30.7	.98	.76
	1.15	85	69	.041	50	55	-53.4	1.7	-8.5	70	40.1	.024	-48.5	32.6	-45.0	.79	-94	.020	-8.5	.64	-53.4	.74	
	1.60	50	19	.032	40	41	-37.2	1.2	11.8	27	63.9	.043	-52.1	35.2	-48.9	1.52	-101	.024	11.8	.92	-37.2	.95	
	.28	732	51	.175	602	661	-14.1	11.2	42.9	184	60.7	.061	-17.8	59.2	-56.9	3.59	-75	.015	42.9	.90	-14.1	.97	
1, EBD	.74	314	69	.160	223	259	-25.4	6.9	13.4	137	54.2	.051	-40.8	37.2	-38.8	1.89	-80	.022	13.4	.82	-25.4	.96	.77
	1.15	85	40	.058	70	74	-41.2	2.1	4.1	57	58.9	.038	-54.8	35.0	-45.2	1.31	-100	.025	4.1	.87	-41.2	.93	
	1.60	50	28	.022	25	32	-44.4	.9	15.5	33	42.3	.028	-26.7	34.4	-59.9	.96	-87	.019	15.5	.67	-44.4	.81	
	.28	712	228	.432	1017	798	-19.6	16.0	38.2	271	98.1	.059	-60.0	50.0	-57.8	2.95	-118	.022	38.2	1.12	-19.6	.84	
8, EBI	.74	320	124	.150	185	214	-29.8	6.2	4.7	163	40.0	.038	-35.3	34.6	-34.5	1.31	-70	.019	4.7	.69	-29.6	.85	.65
	1.15	98	154	.147	182	117	-59.0	3.6	-15.0	108	69.4	.034	-84.5	32.2	-43.9	1.08	-128	.037	-15.0	1.19	-59.7	.91	
	1.60	45	46	.023	45	29	-61.2	.7	-13.0	37	42.3	.018	-55.3	43.6	-48.2	.78	-104	.016	-13.0	.70	-60.6	.81	

NOTE: Spectral data shown are actual spectra times 50. Rounding off the data may account for minor inconsistencies in data presented.

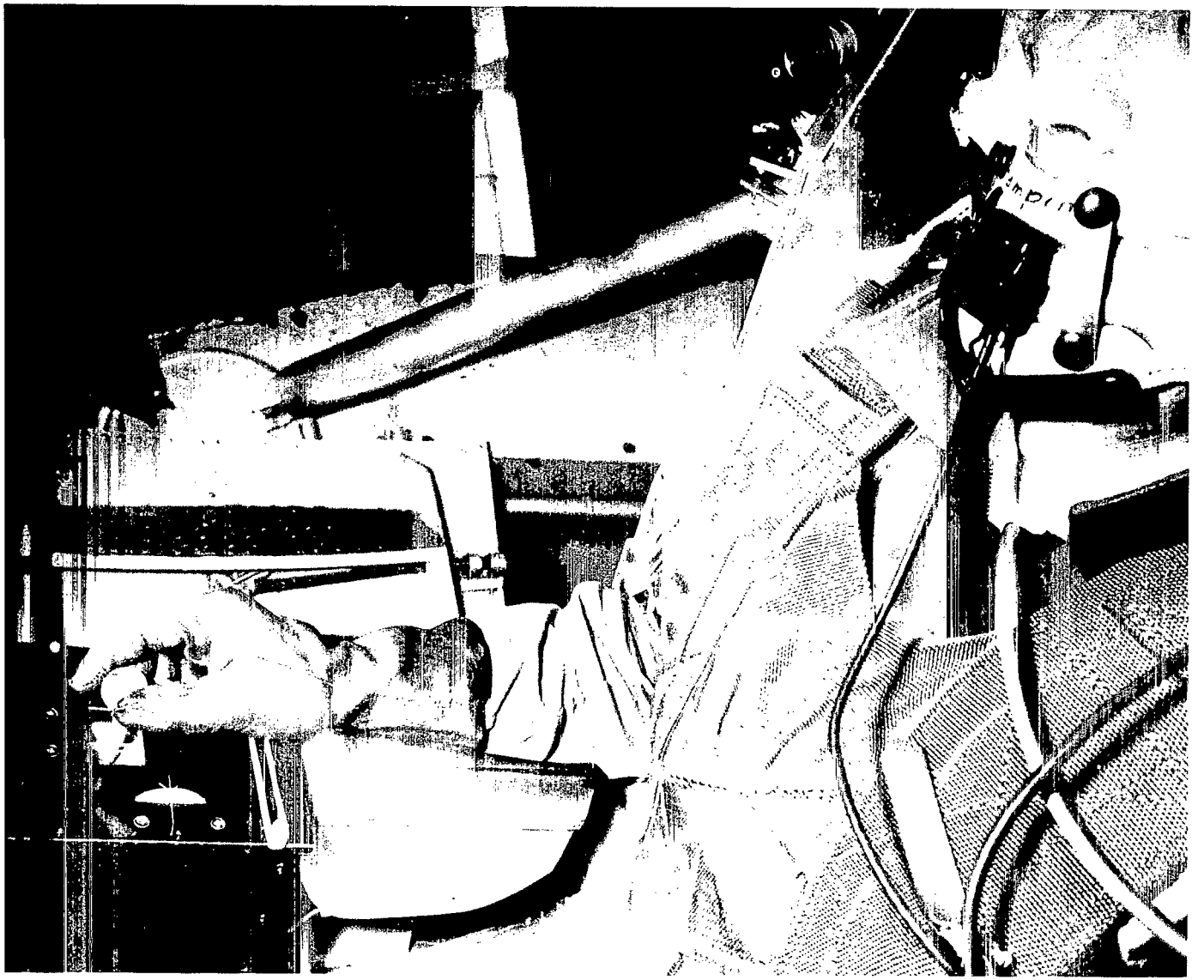

A-25822

(a) Pencil controller.

Figure 1.- Photographs of controls.

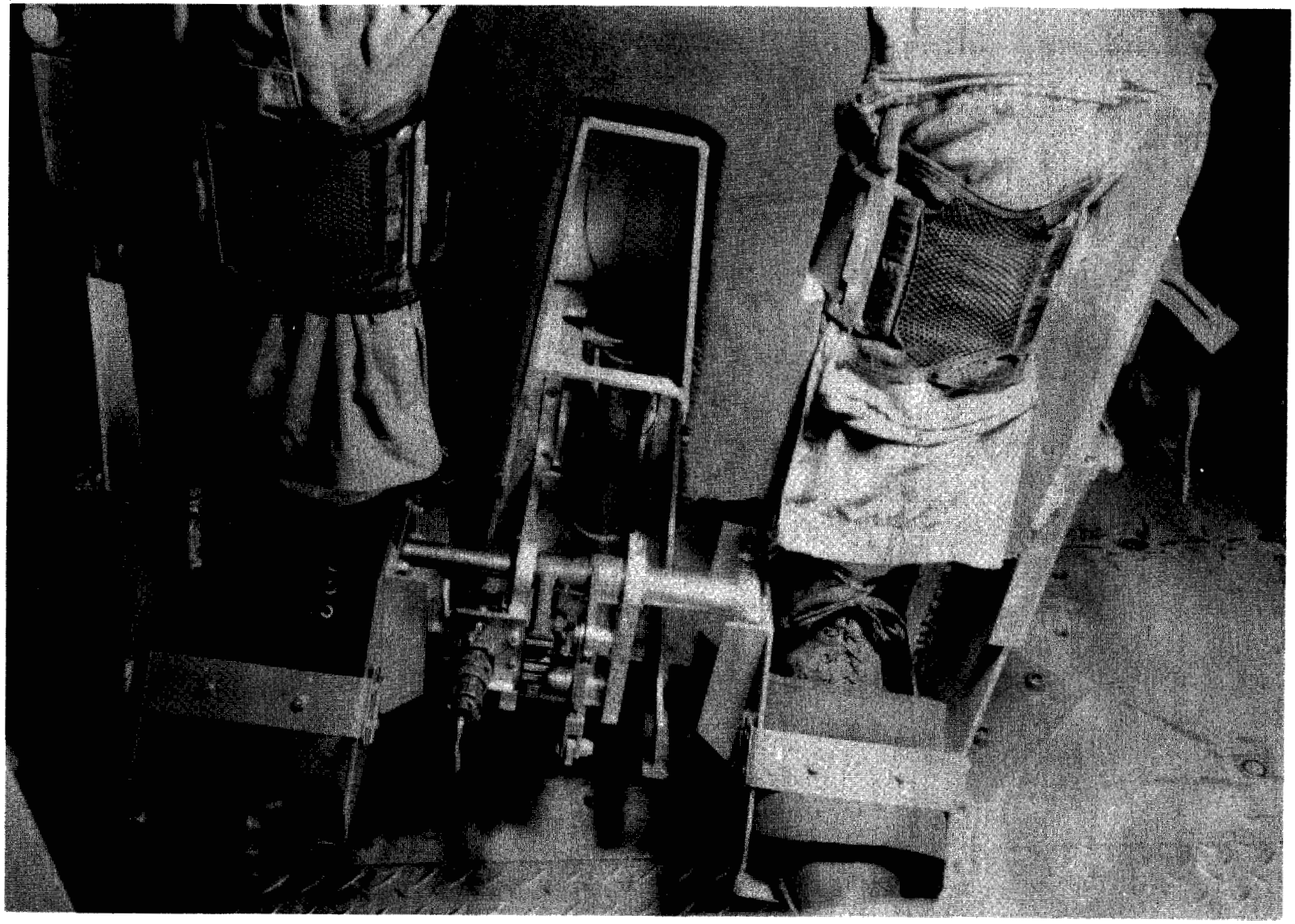

(b) Toe pedals.

A-25988

Figure 1.- Concluded.

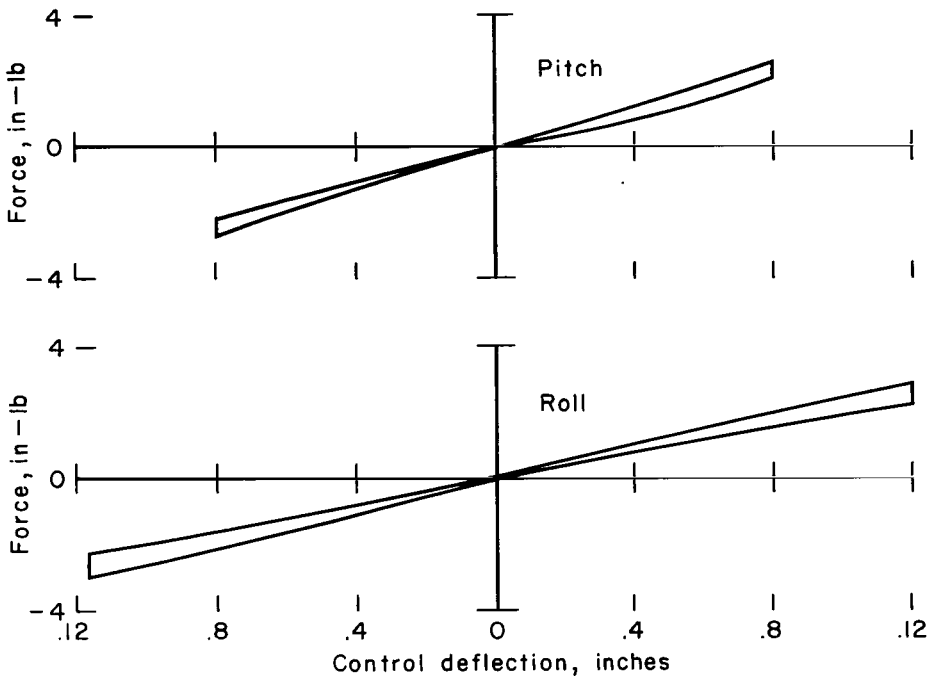

(a) Pencil controller.

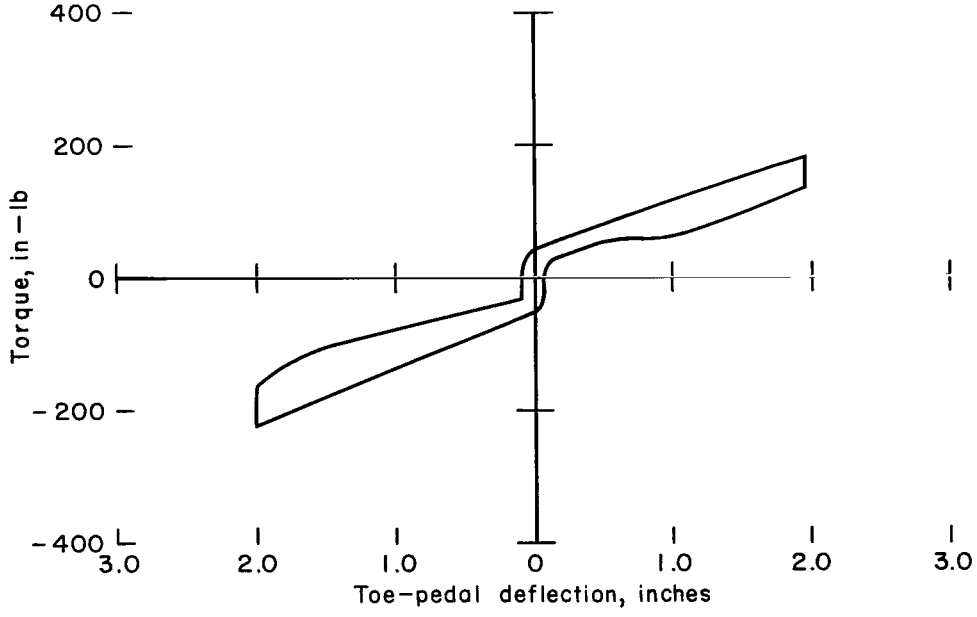

(b) Toe pedals.

Figure 2.- Force deflection characteristics of pilot controls.

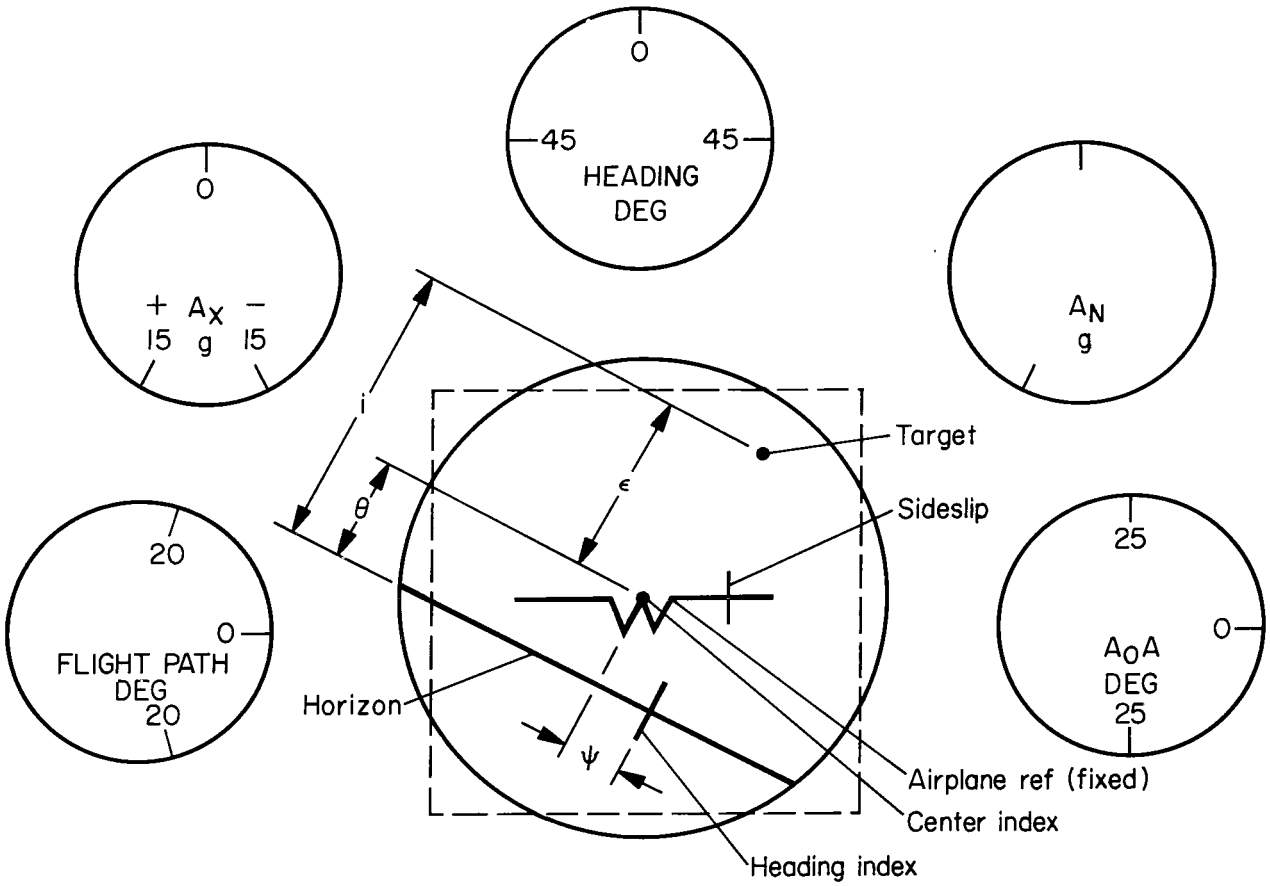

Figure 3.- Pilot's display.

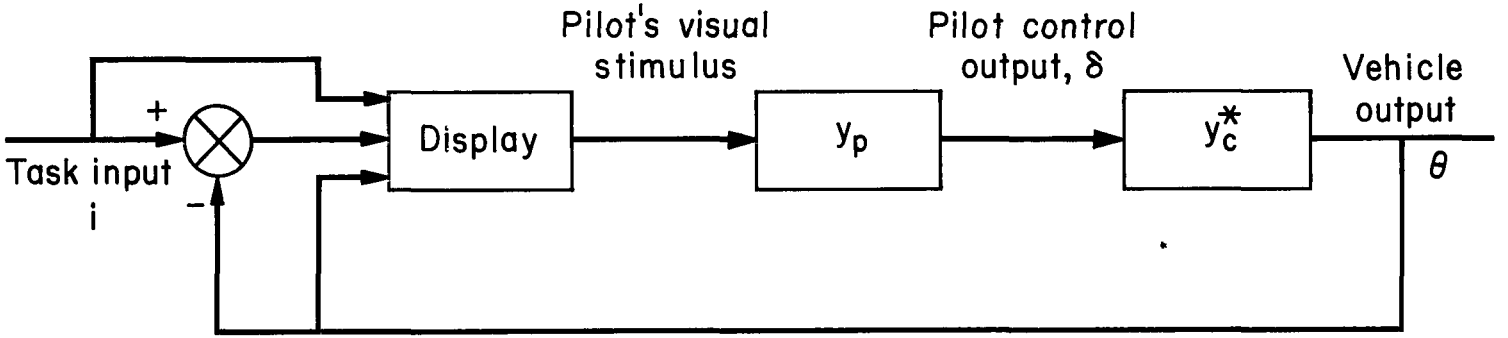

$$*y_c(s) = K_c \frac{(1 + T_\theta S)}{S\left[\frac{S^2}{\omega_n^2} + \frac{2\xi S}{\omega_n} + 1\right]} = 13.4 \frac{(1 + 2.3S)}{S\left[\frac{S^2}{11.25} + \frac{2(.53)S}{3.35} + 1\right]}$$

Figure 4.- Block diagram of primary pitch-attitude control task.

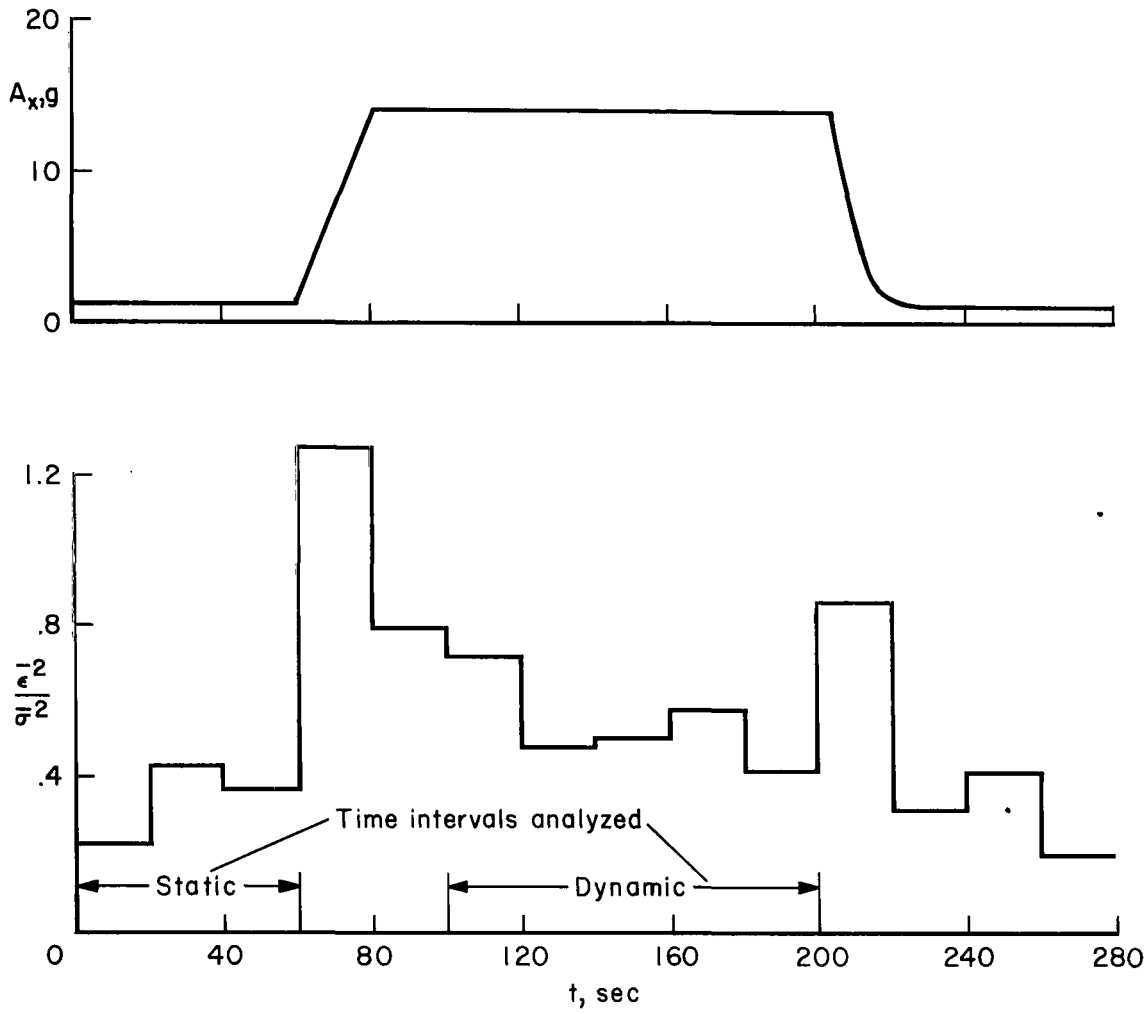

Figure 5.- Typical acceleration profile and associated control task performance (pilot B).

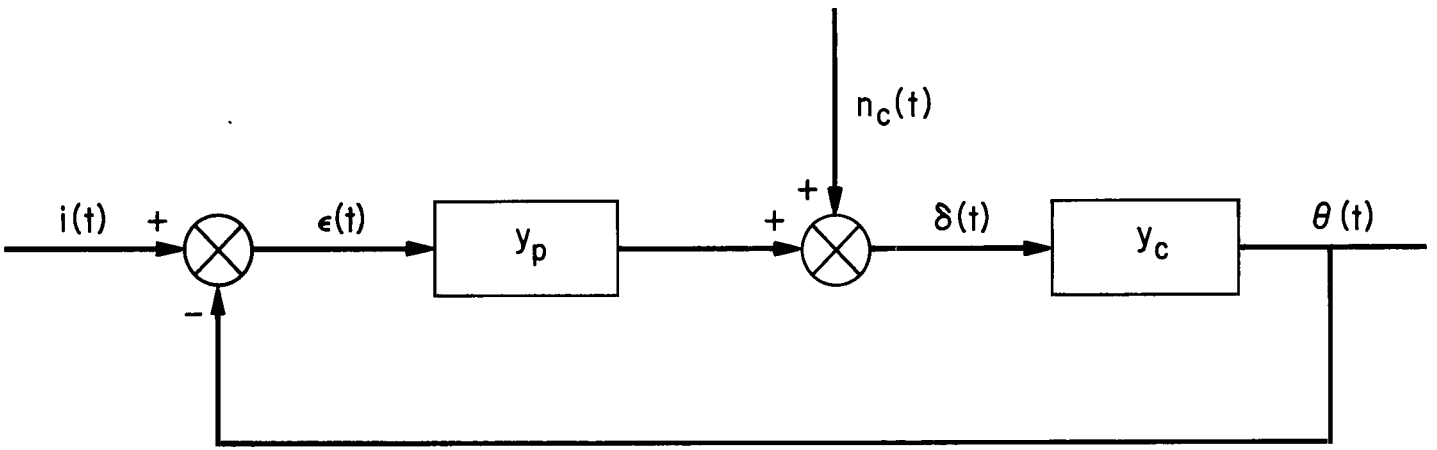

Figure 6.- Block diagram of equivalent compensatory system analyzed.

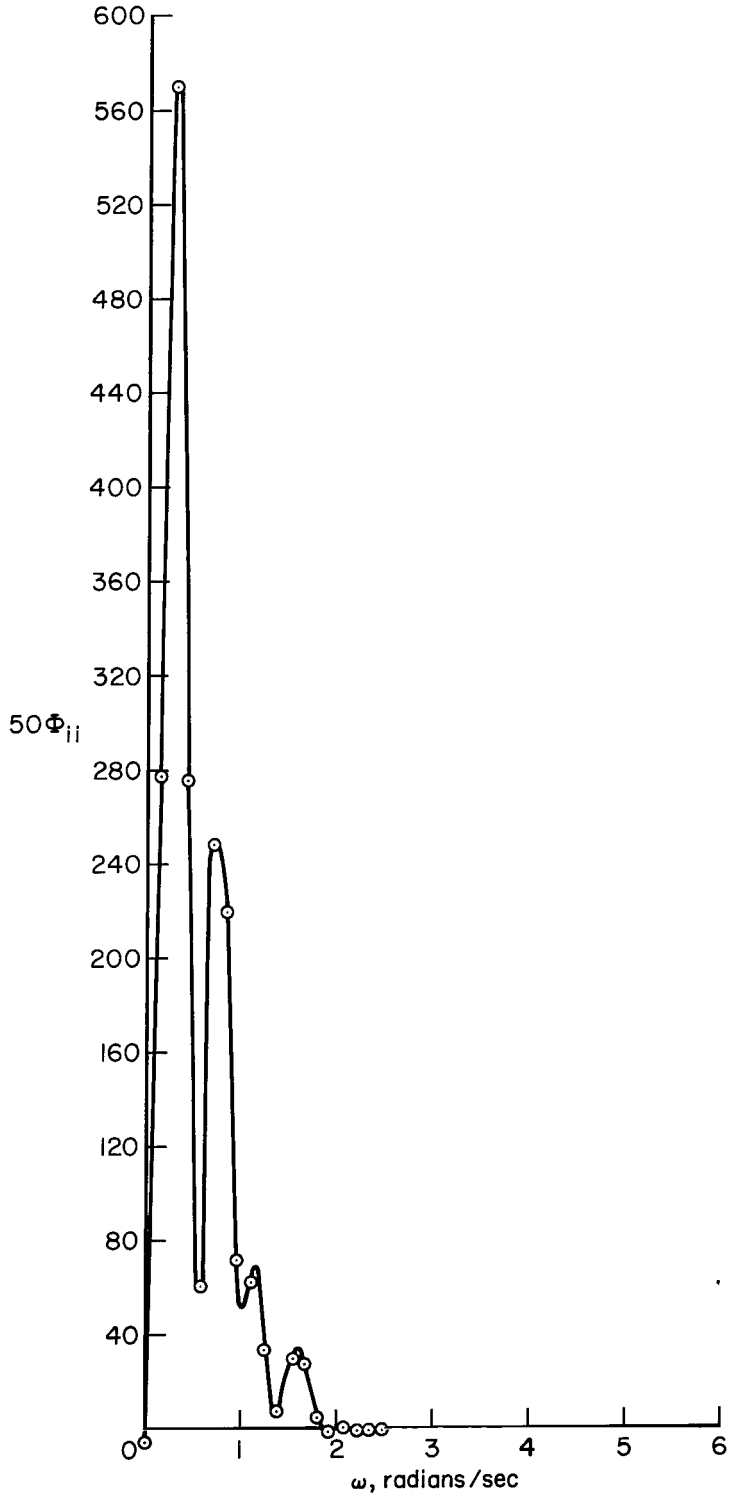

(a) Φ_{ii}

Figure 7.- Typical set of spectra (pilot C, 1 g).

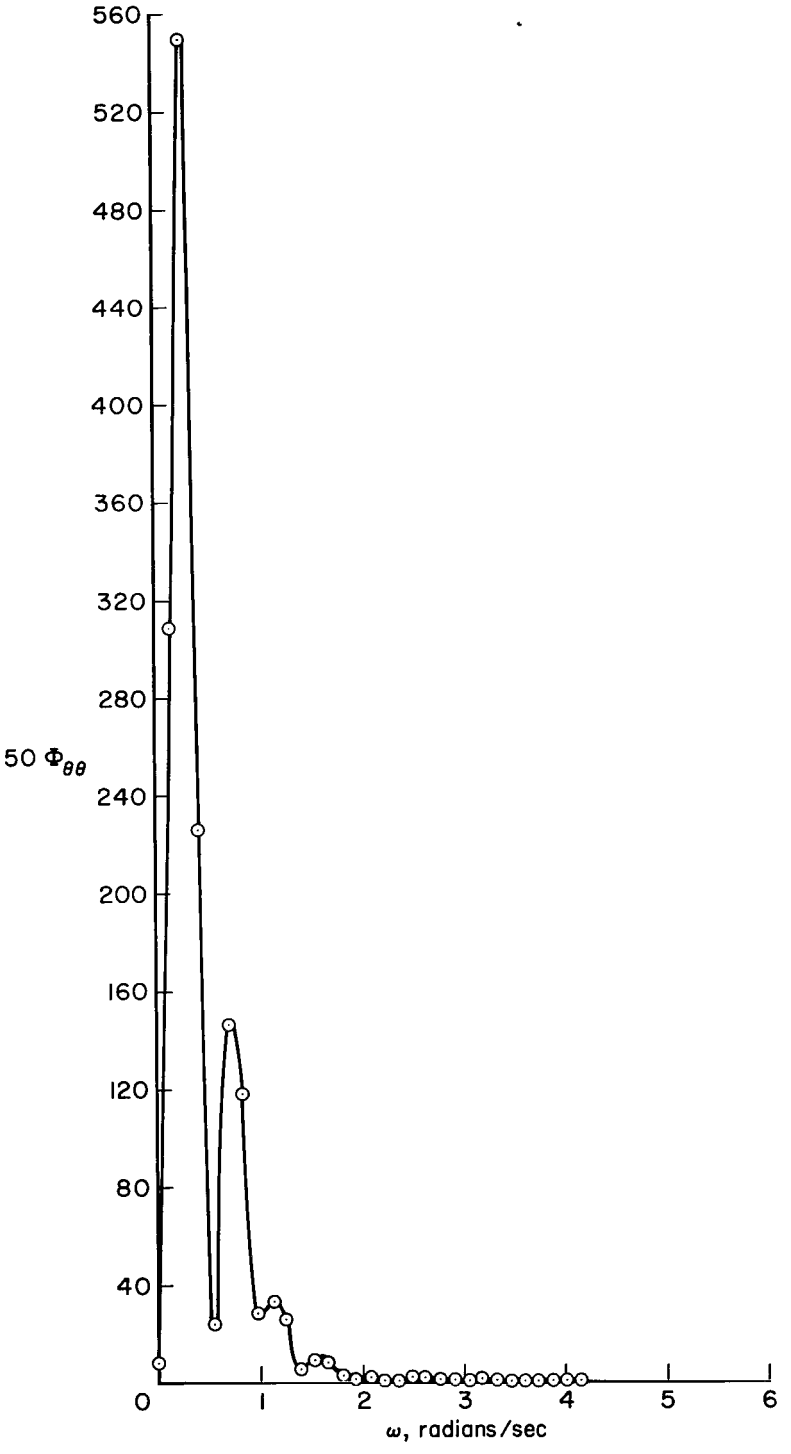

(b) $\Phi_{\theta\theta}$

Figure 7.- Continued.

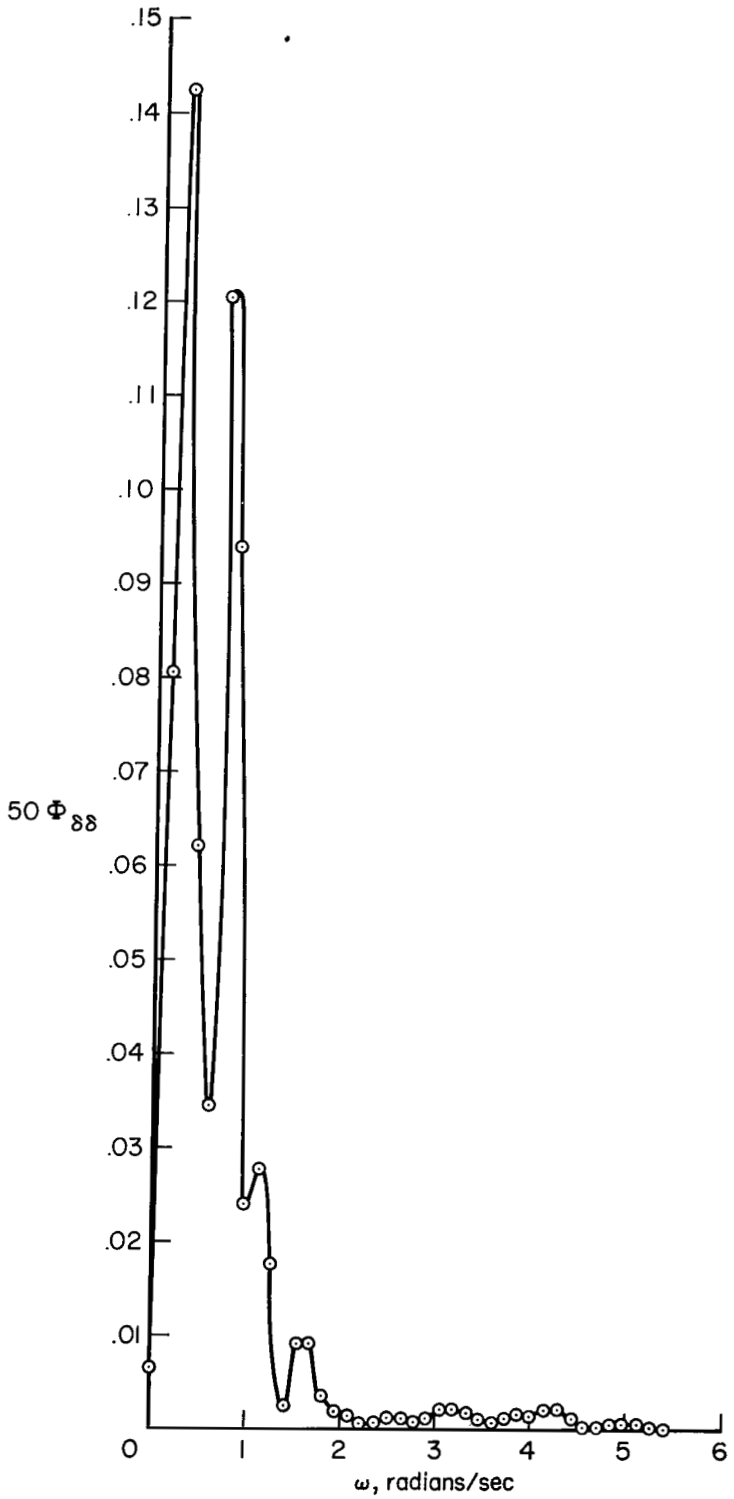

(c) $\Phi_{\delta\delta}$

Figure 7.- Continued.

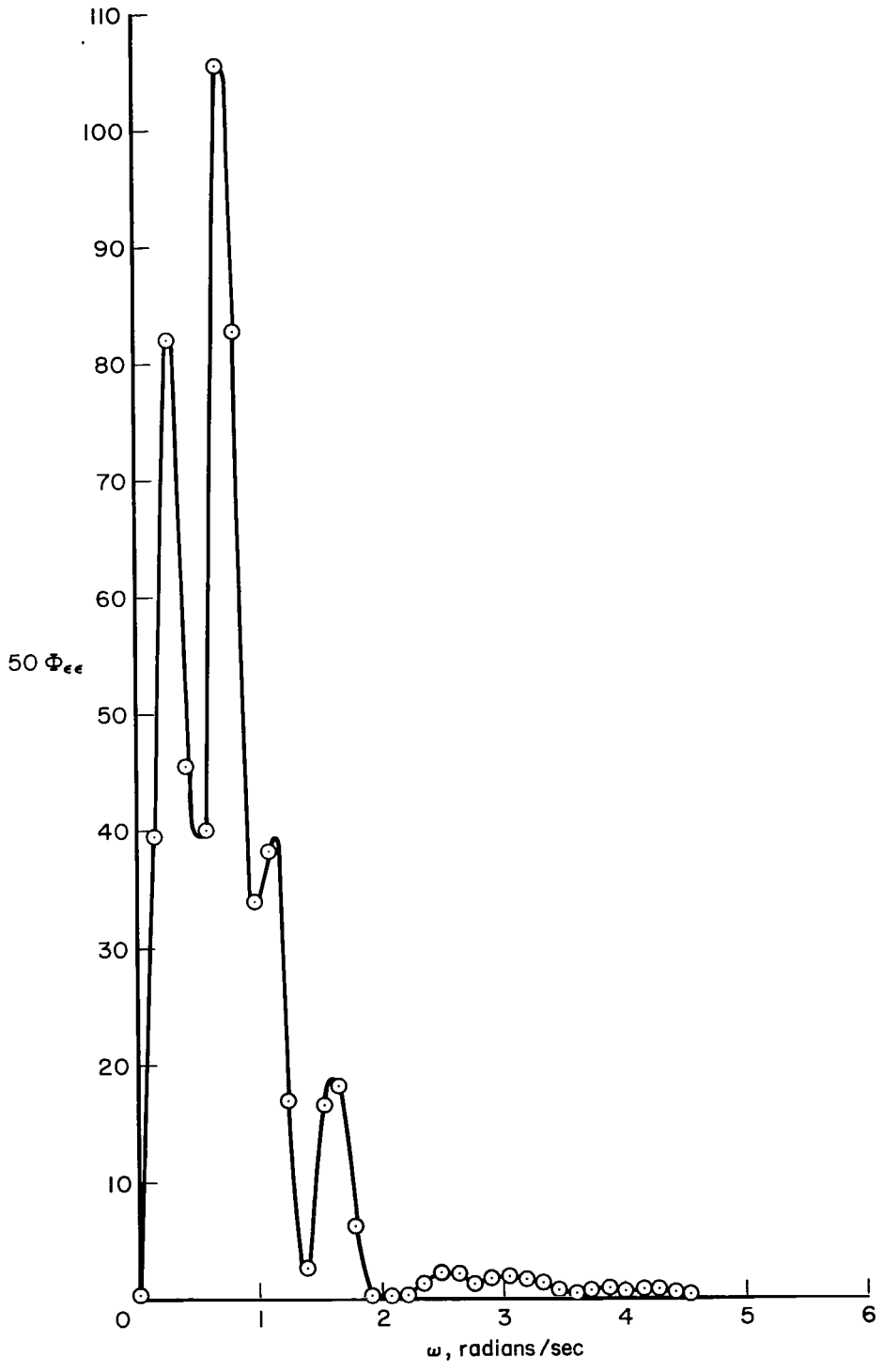

(d) $\Phi_{\epsilon\epsilon}$

Figure 7.- Continued.

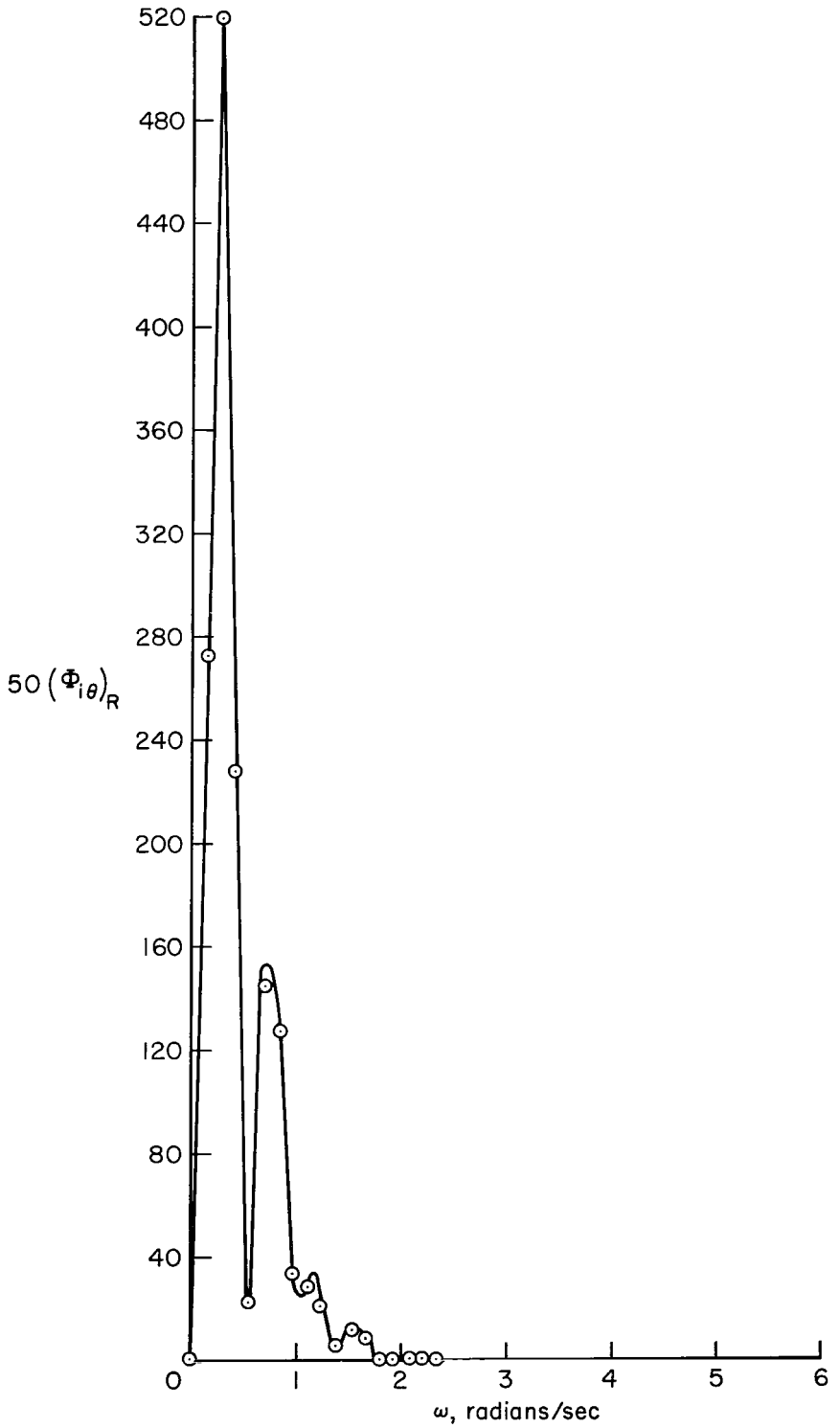

(e) $(\Phi_{i\theta})_R$

Figure 7.- Continued

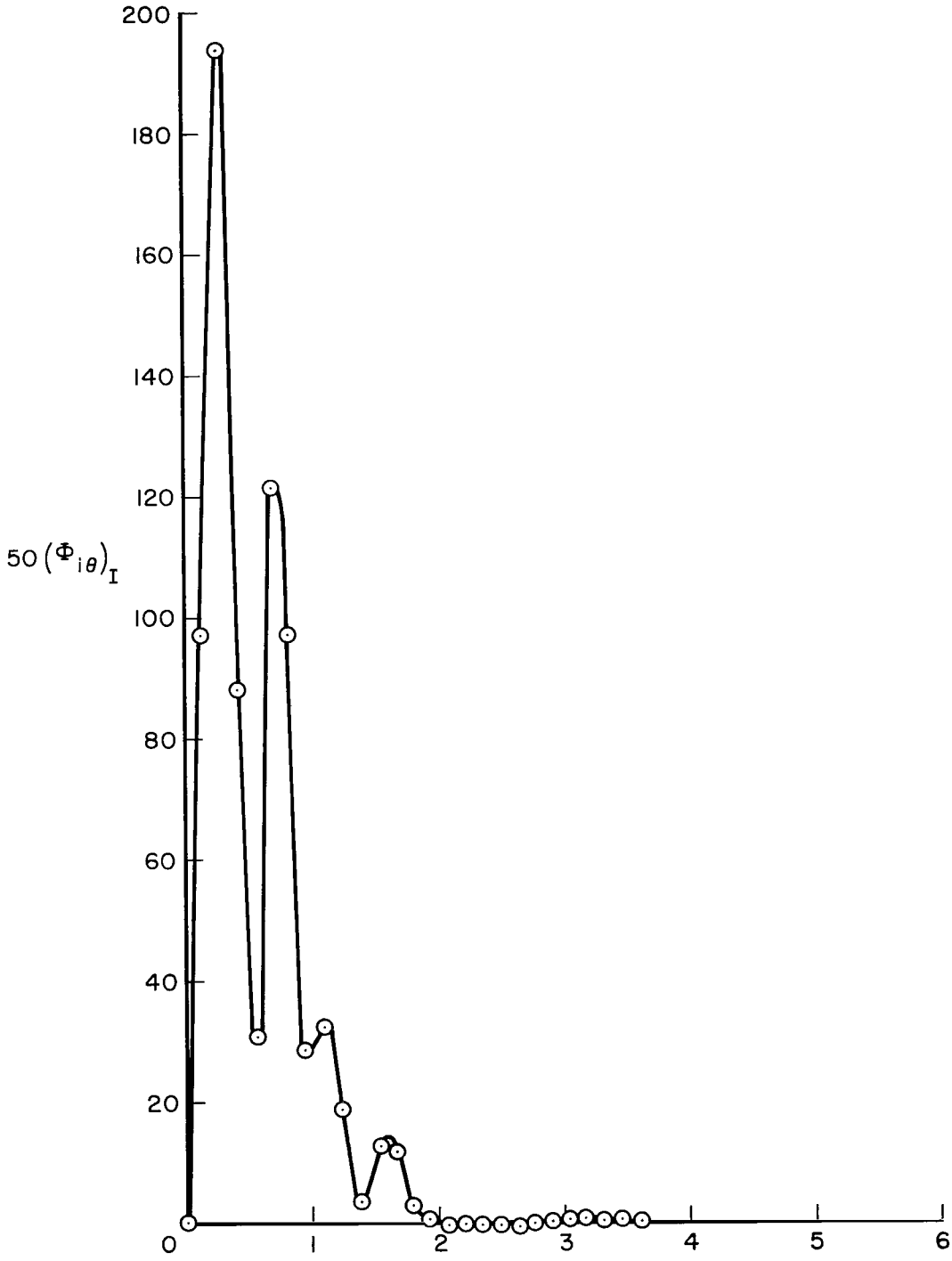

(f) $(\Phi_{i\theta})_I$

Figure 7.- Continued.

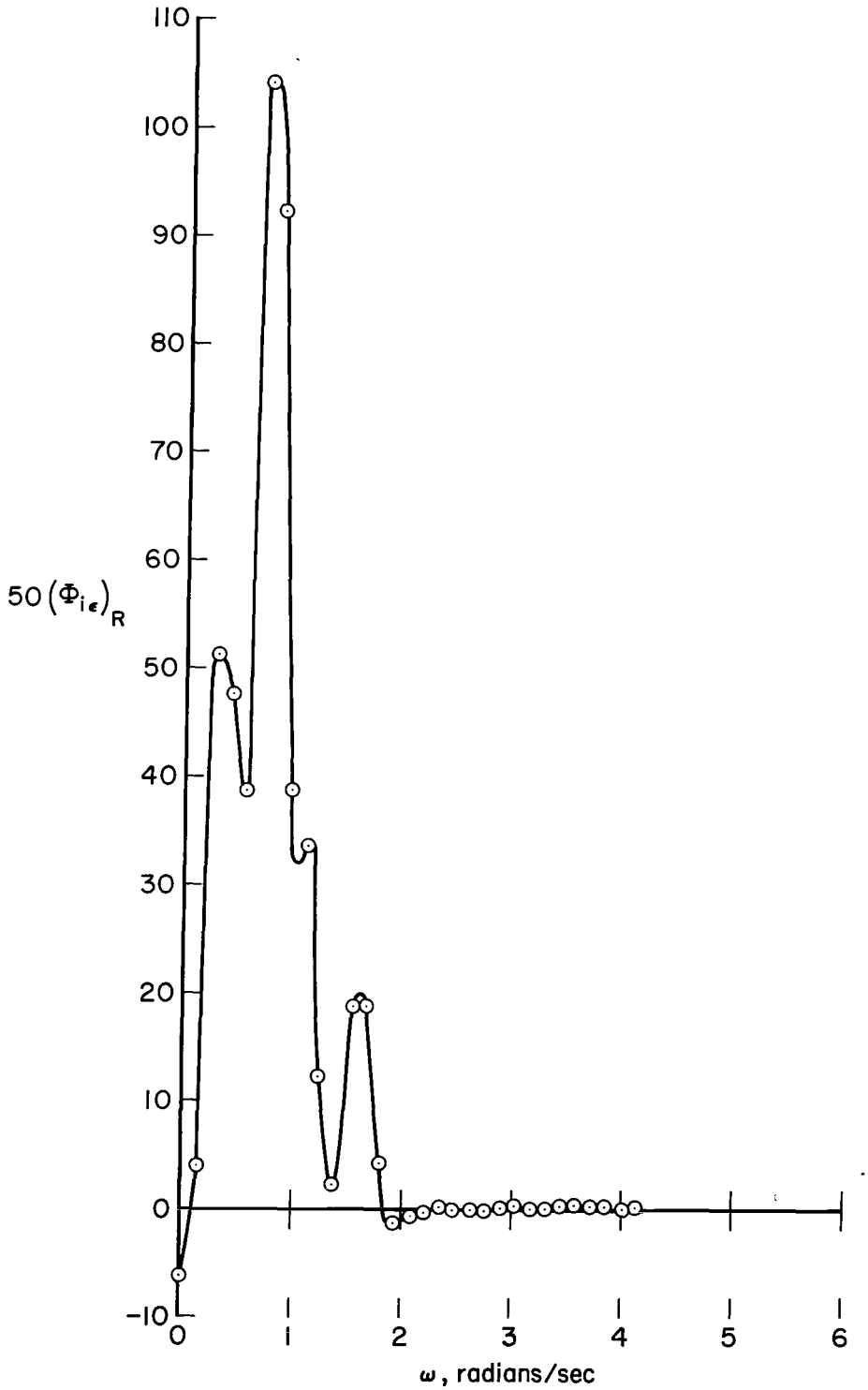

(g) $(\Phi_{i\epsilon})_R$

Figure 7.- Continued.

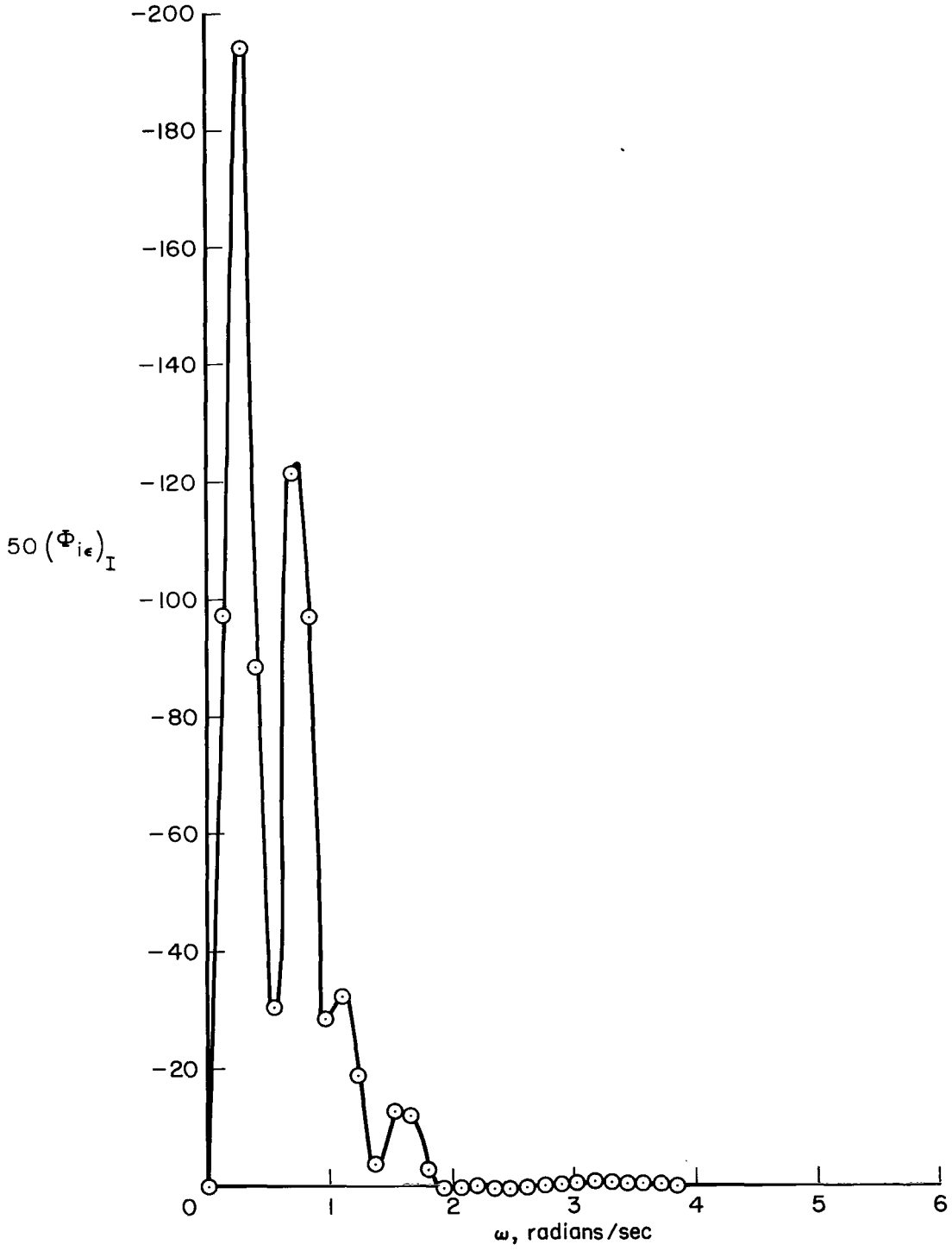

(h) $(\Phi_{i\epsilon})_I$

Figure 7.- Continued.

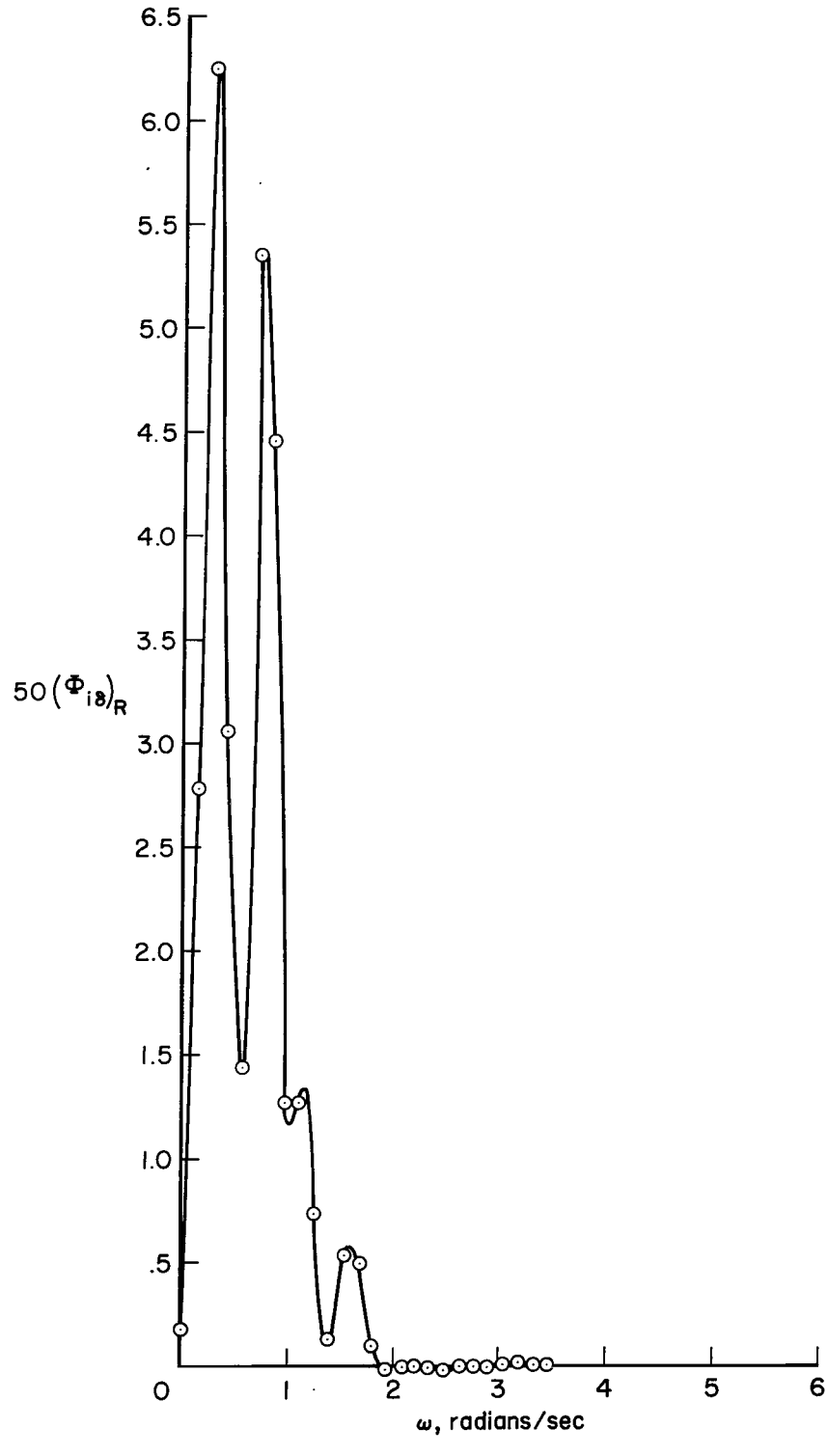

(i) $(\Phi_{i\delta})_R$

Figure 7.- Continued.

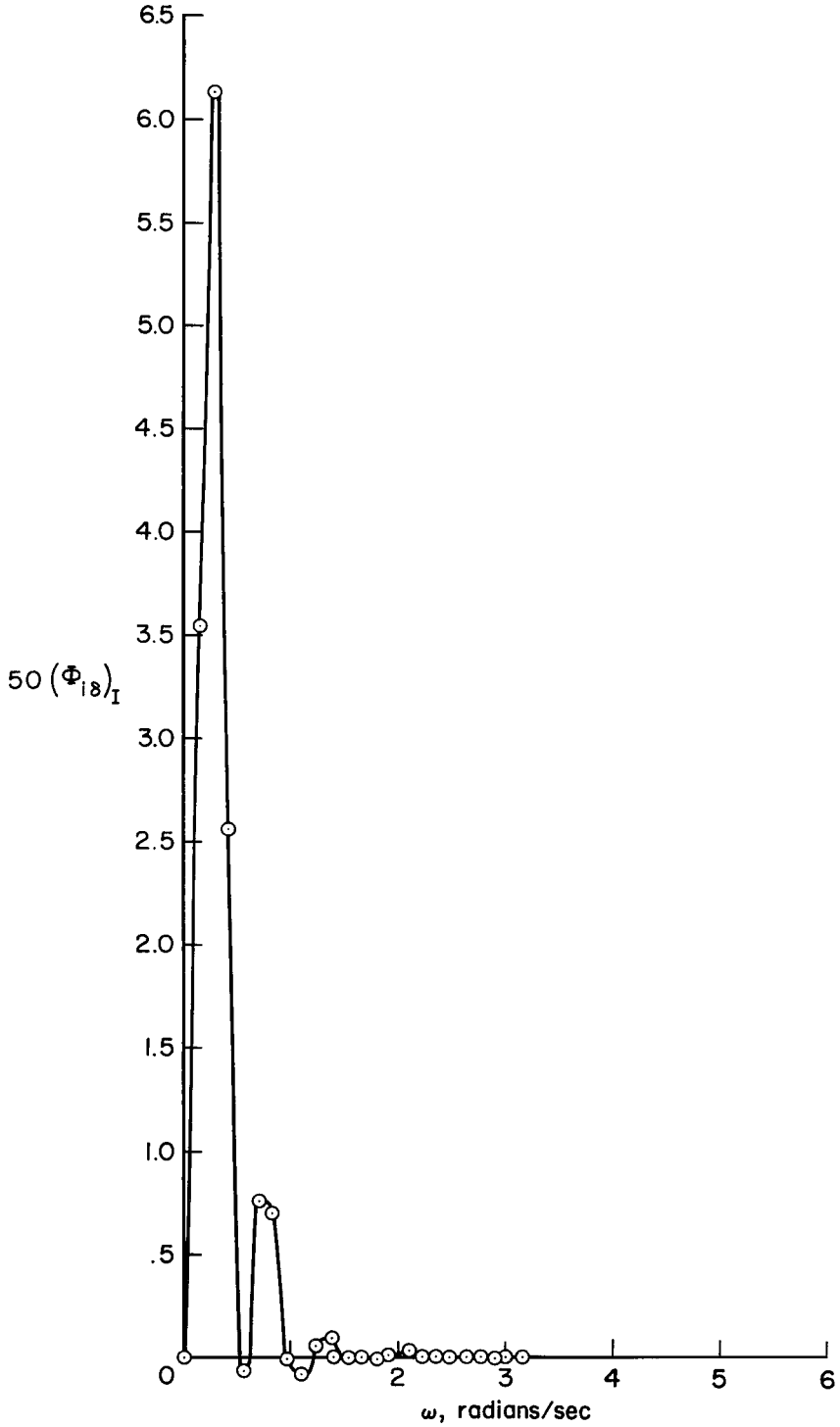

(j) $(\Phi_{i\delta})_I$

Figure 7.- Concluded.

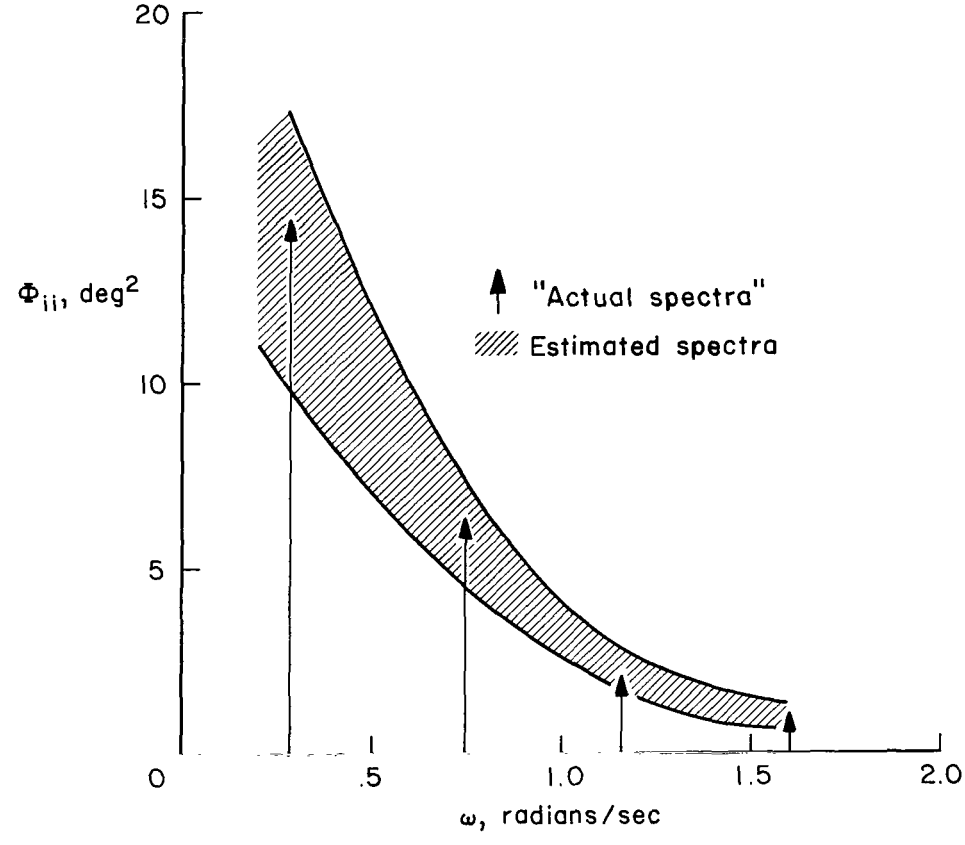

(a) Input spectra.

Figure 8.- Comparison between actual and computed input spectra and vehicle transfer function.

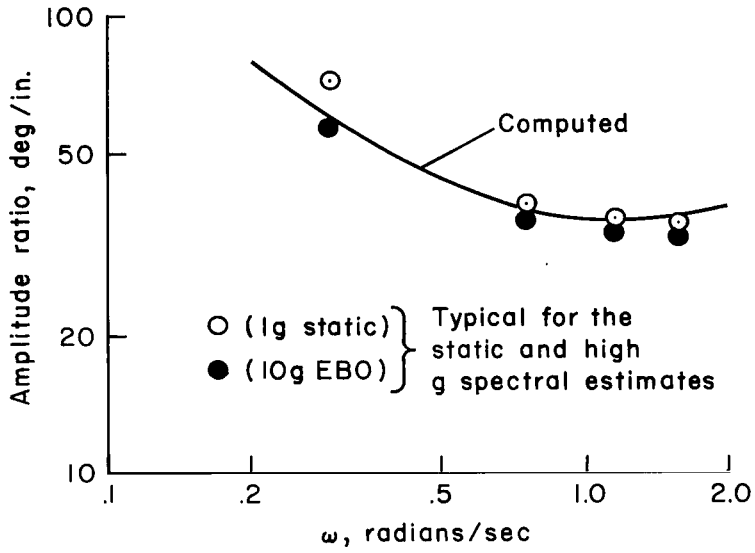

(b) Amplitude, Y_c.

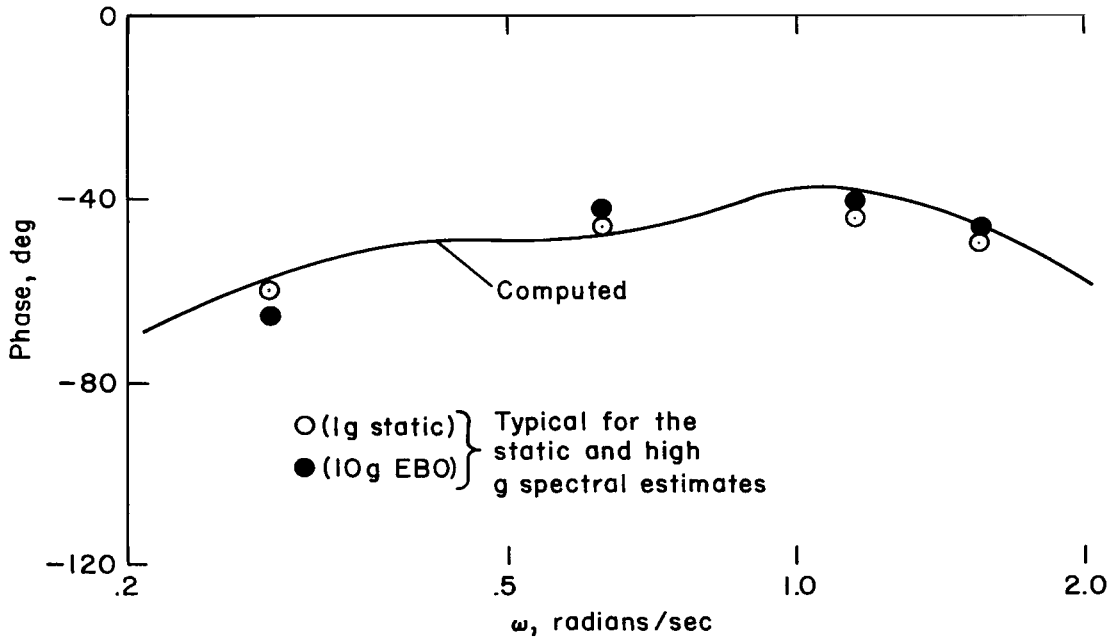

(c) Phase, Y_c.

Figure 8.- Concluded.

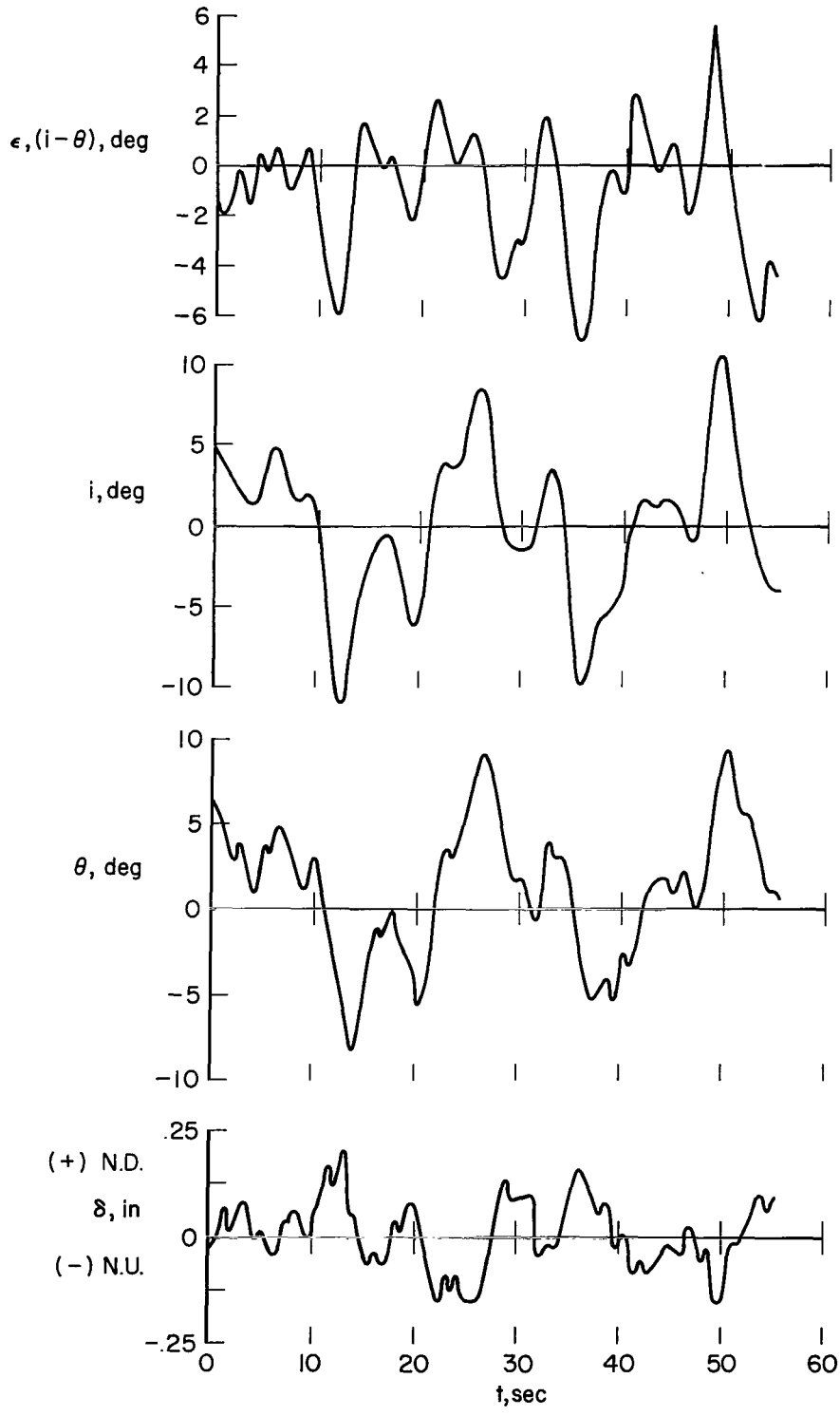

(a) Static, 1 g.

Figure 9.- Typical time history of tracking run (pilot C).

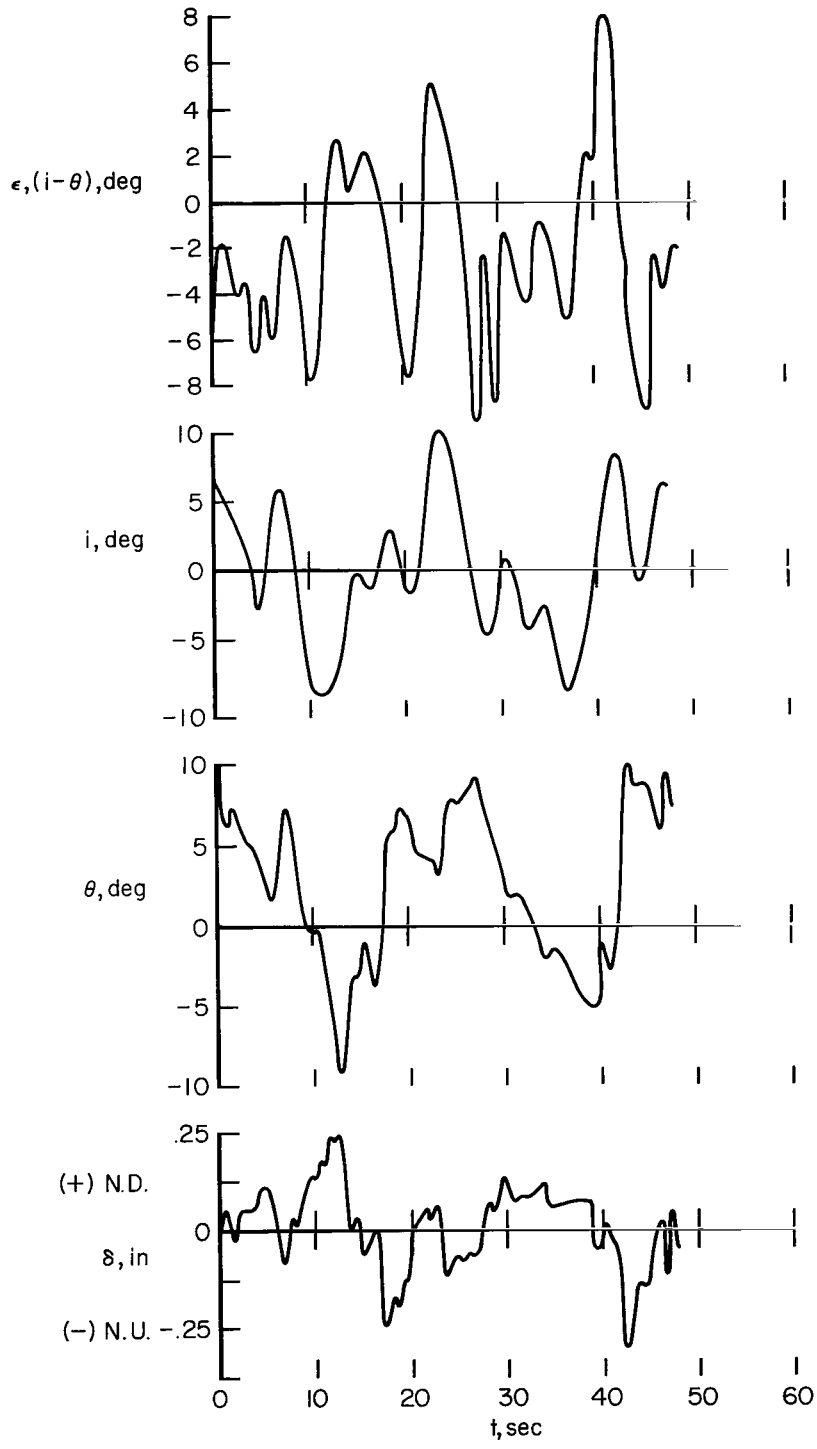

(b) 7 g EBD

Figure 9.- Concluded.

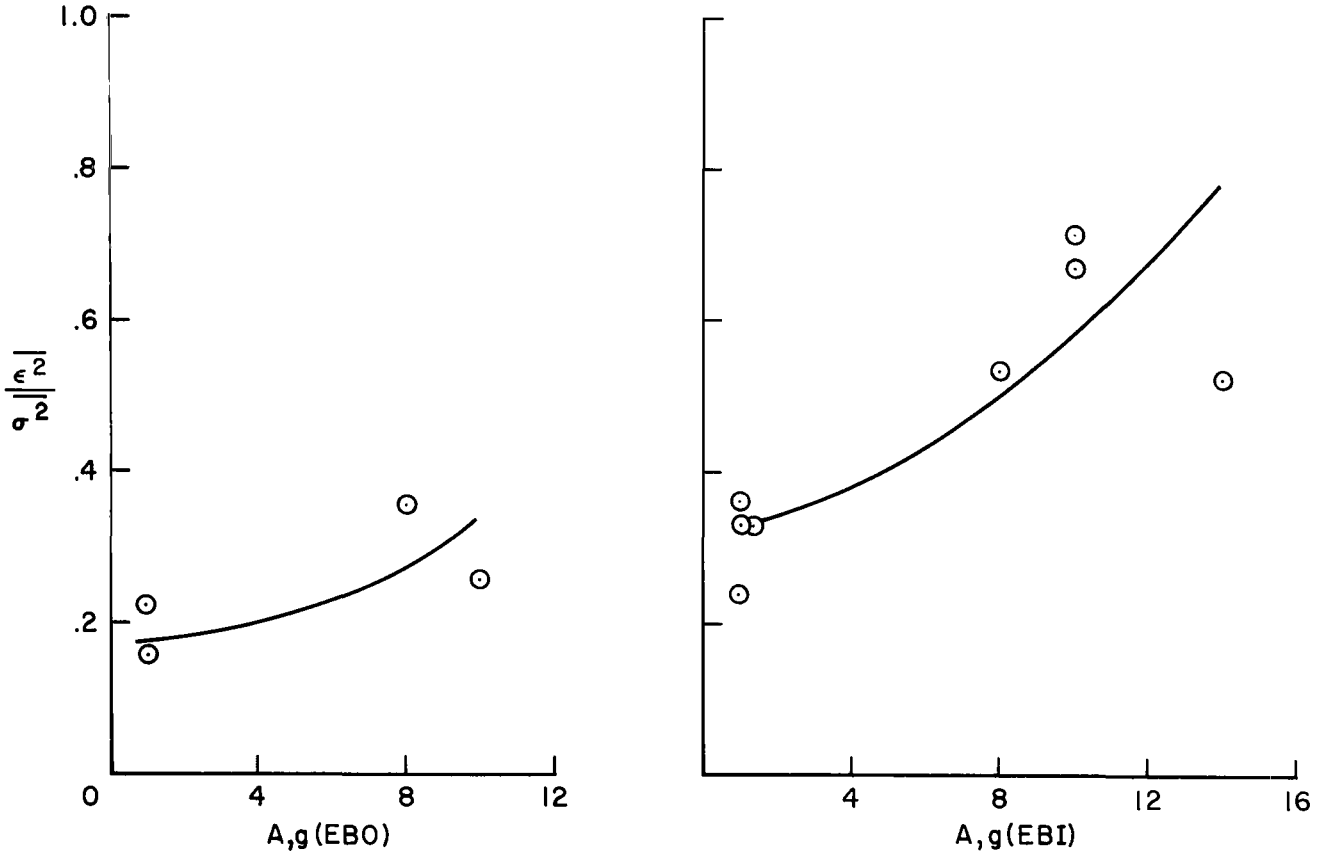

(a) Pilot A.

(b) Pilot B.

Figure 10.- Effects of acceleration on total task performance.

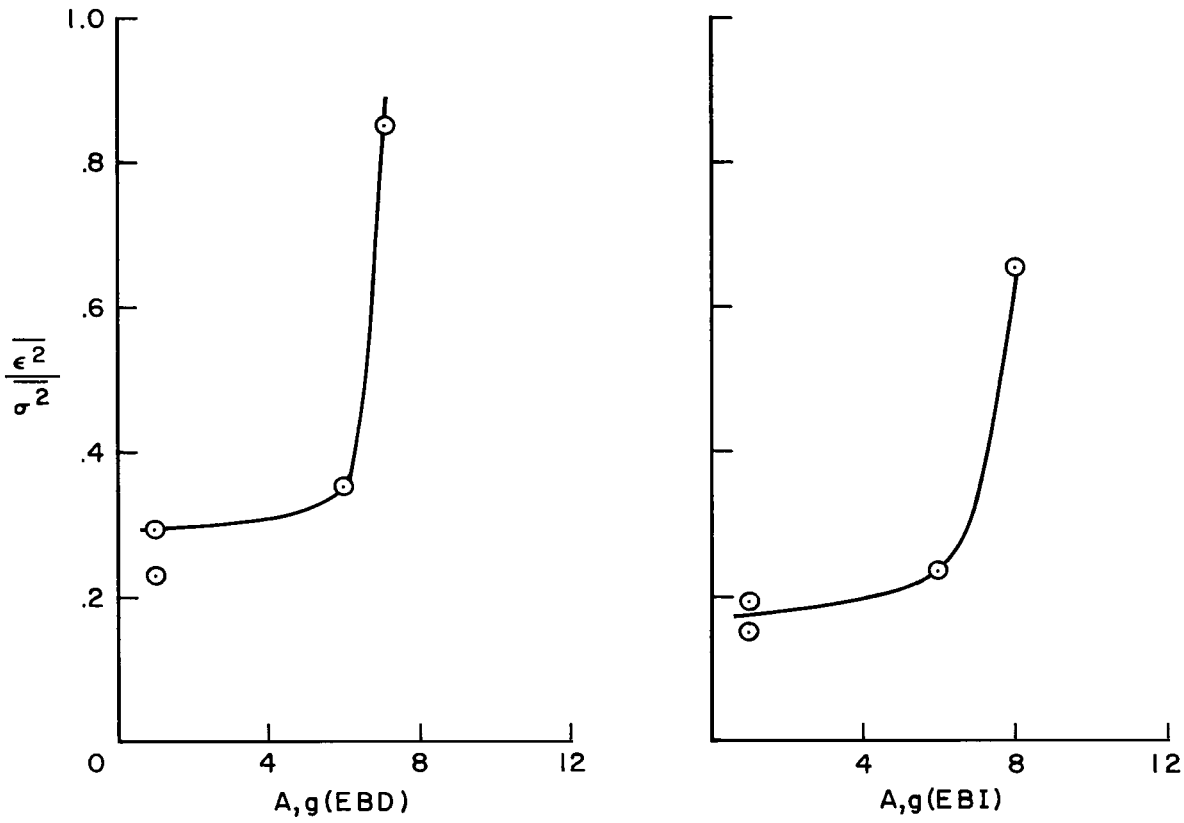

(c) Pilot C.

(d) Pilot D.

Figure 10.- Concluded.

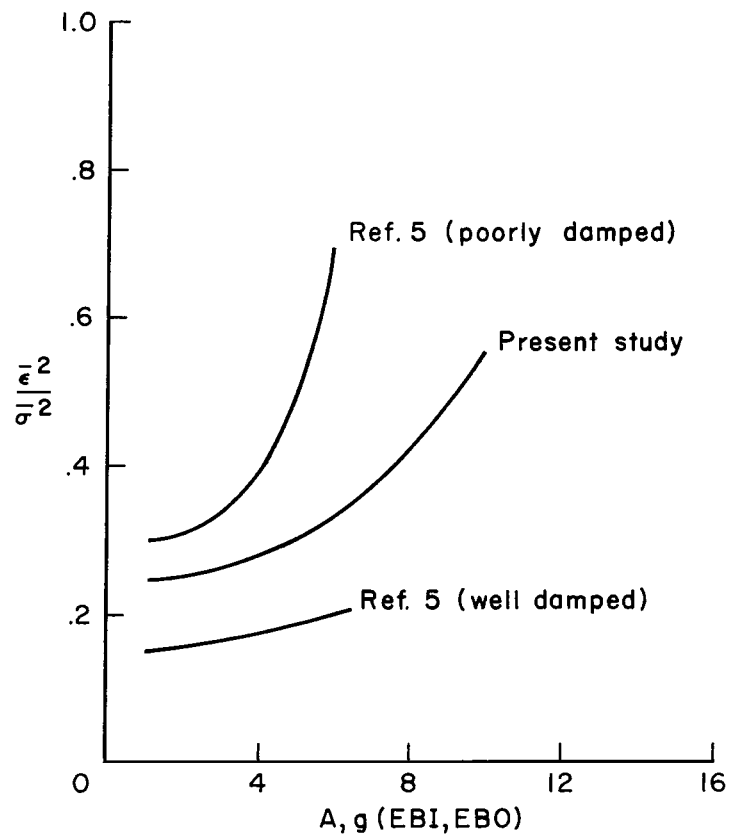

Figure 11.- Comparison of average total task performance with previous results.

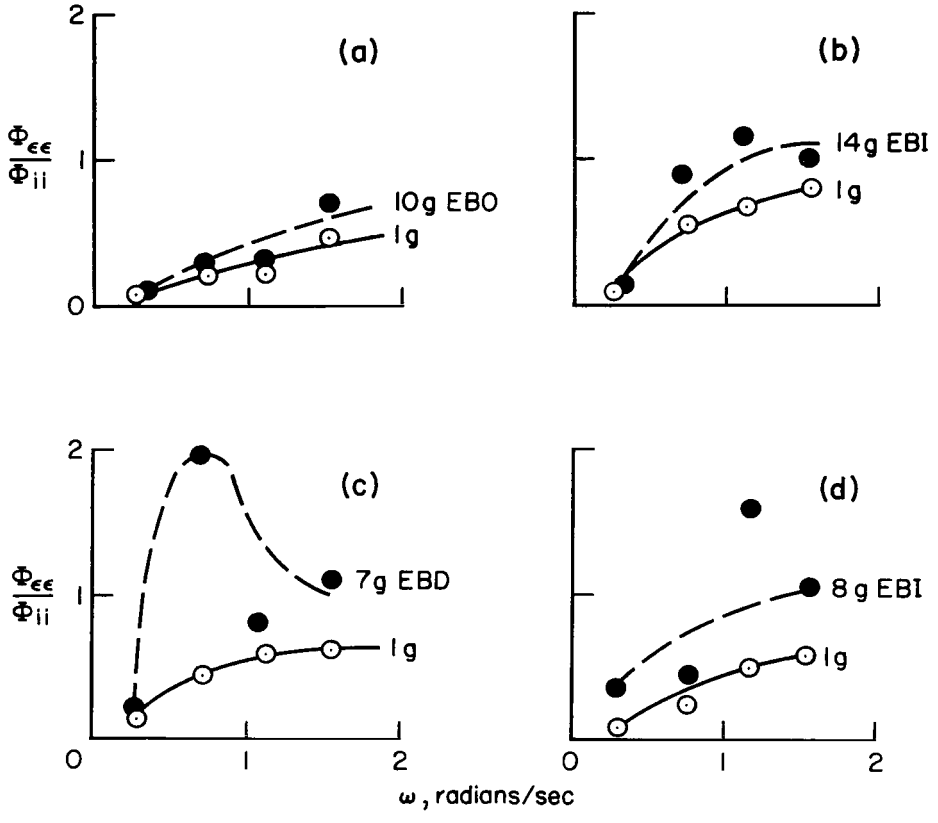

(a) Pilot A. (b) Pilot B.
(c) Pilot C. (d) Pilot D.

Figure 12.- Effects of acceleration on component-task performance.

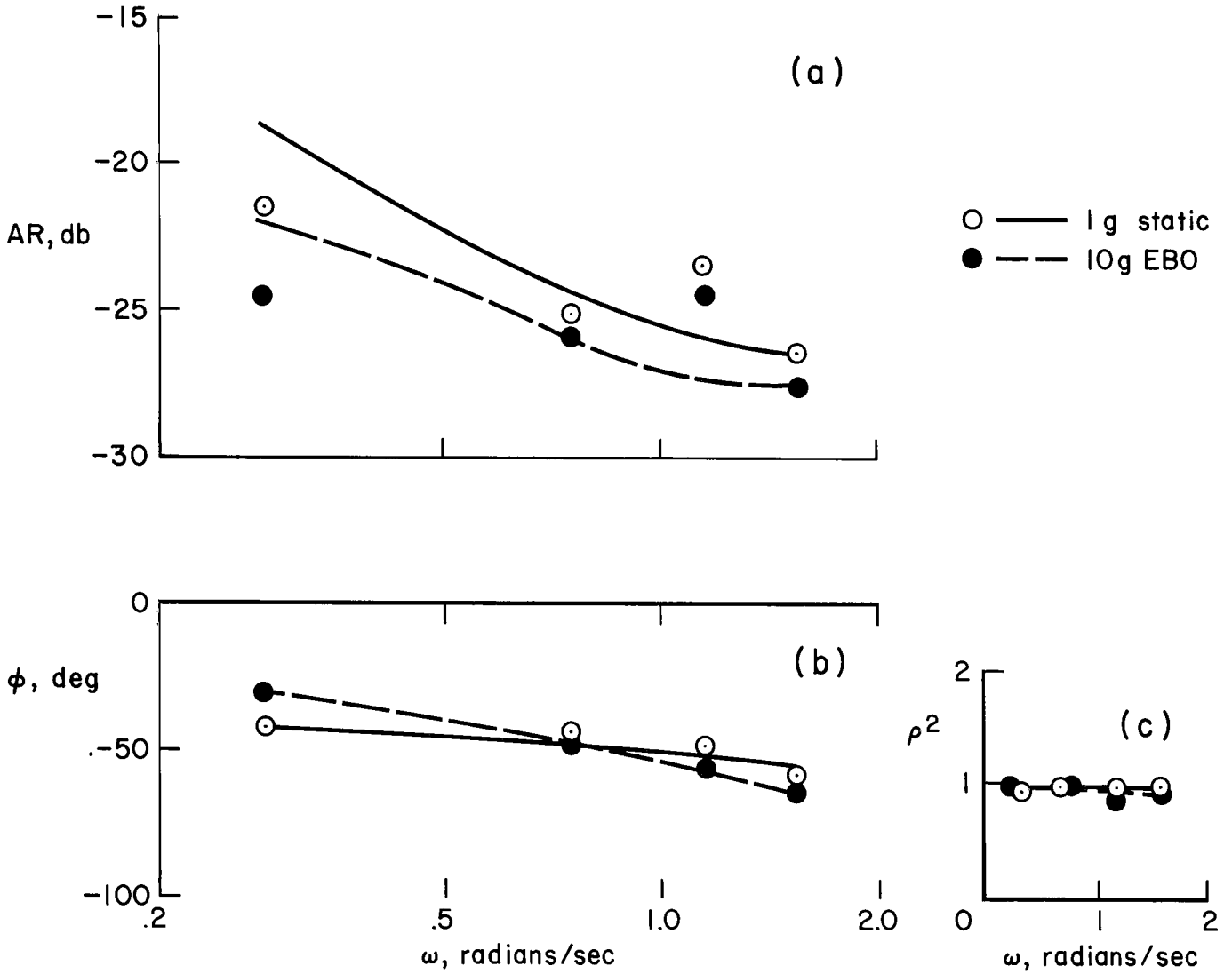

(a) Amplitude ratio, Y_p.
(b) Phase, Y_p.
(c) Linear correlation.

Figure 13.- Effects of acceleration on dynamic response of pilot A.

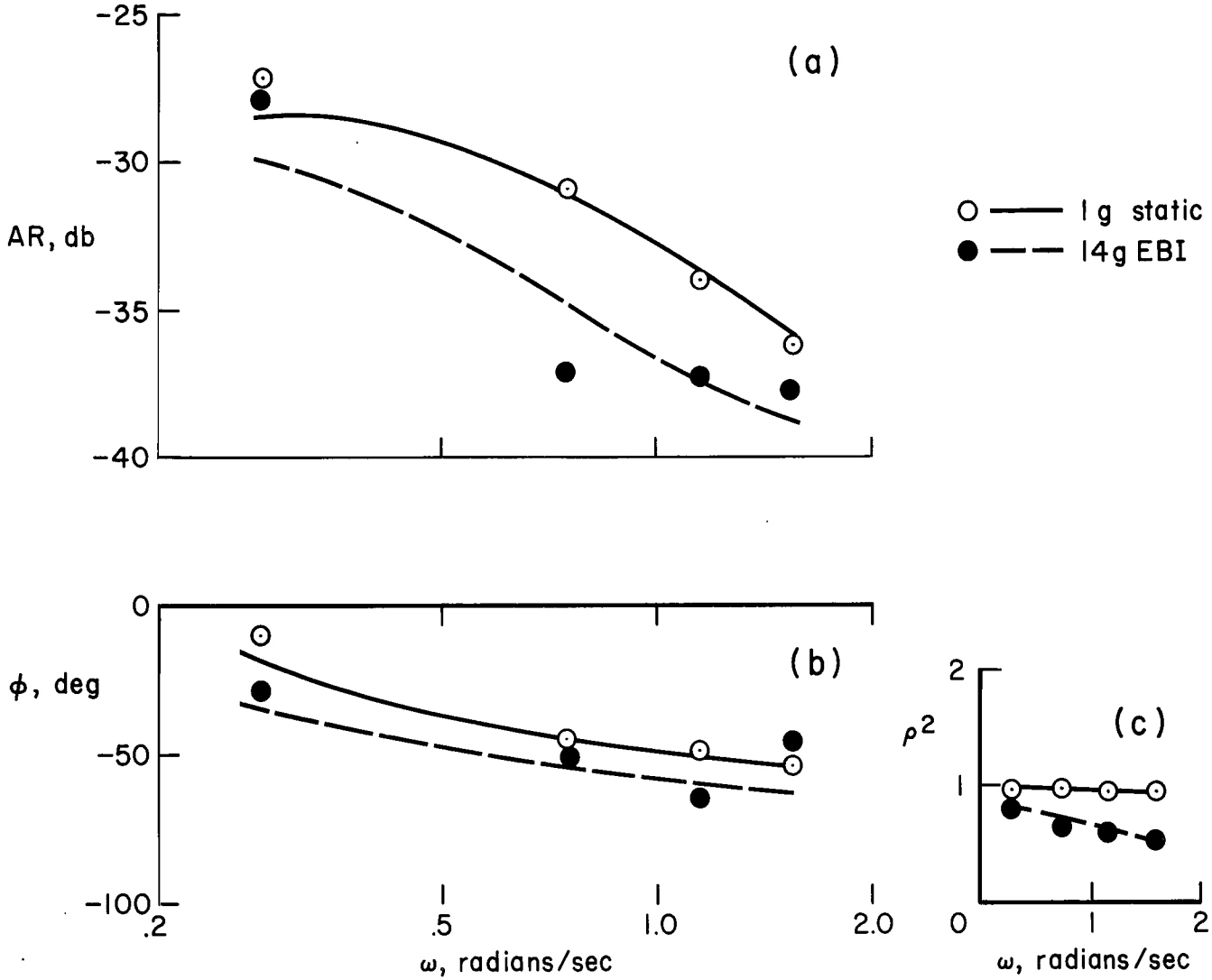

(a) Amplitude ratio, Y_p.
(b) Phase, Y_p.
(c) Linear correlation.

Figure 14.- Effects of acceleration on dynamic response of pilot B.

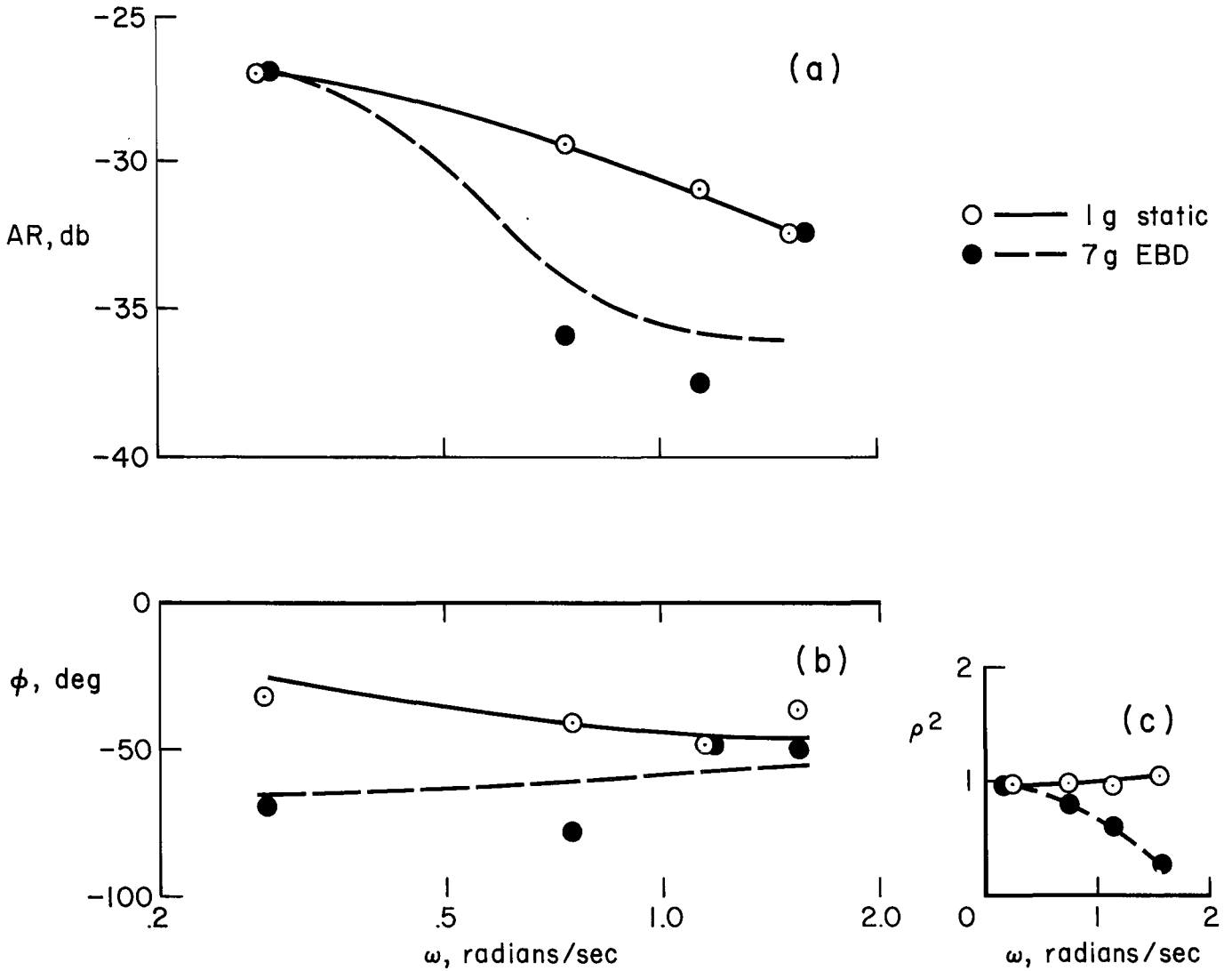

(a) Amplitude ratio, Y_p.
(b) Phase, Y_p.
(c) Linear correlation.

Figure 15.- Effects of acceleration on dynamic response of pilot C.

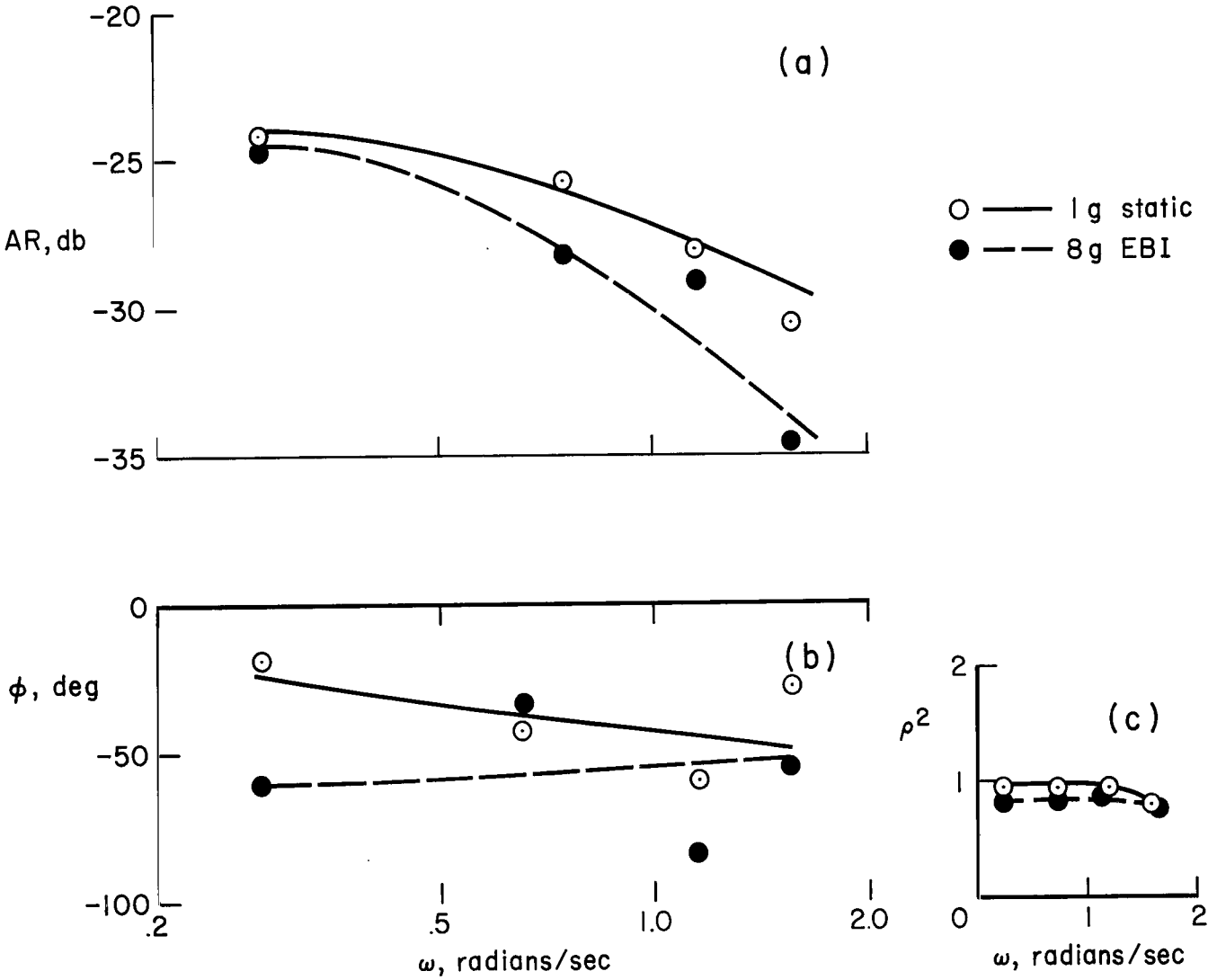

(a) Amplitude ratio, Y_p.
(b) Phase, Y_p.
(c) Linear correlation.

Figure 16.- Effects of acceleration on dynamic response of pilot D.

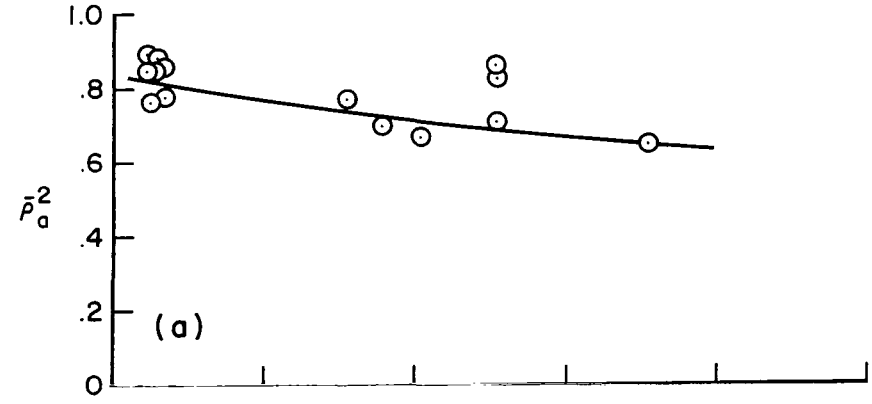

(a) Average linear coherence.

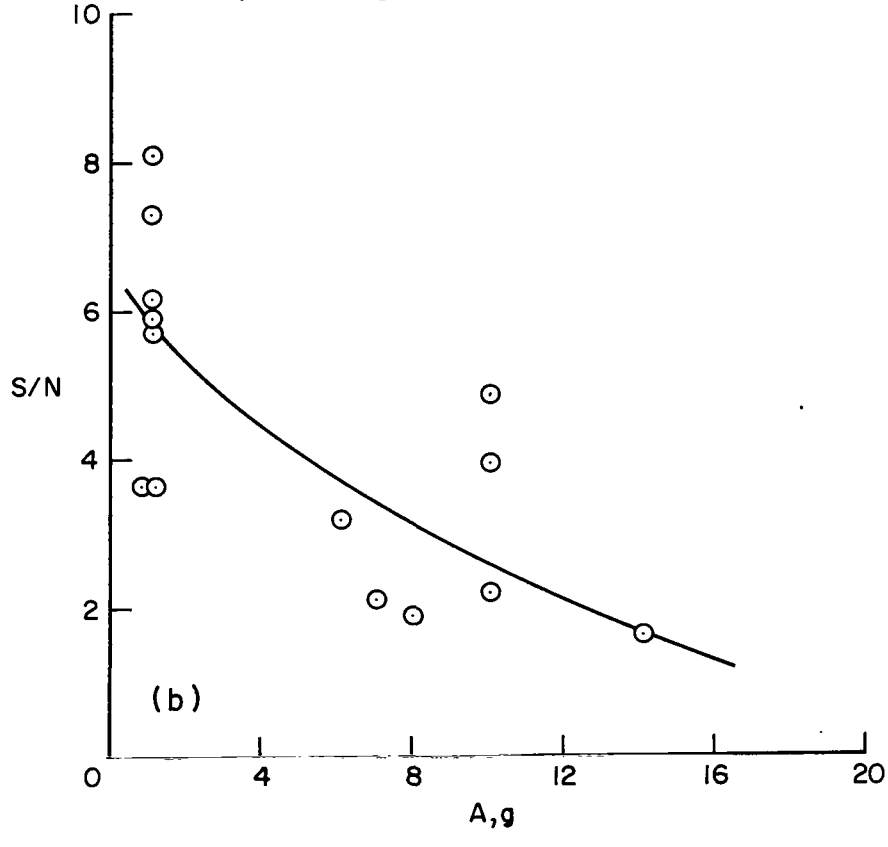

(b) Signal-to-noise ratio.

Figure 17.- Average linear coherence and pilot control signal-to-noise ratio as a function of acceleration.

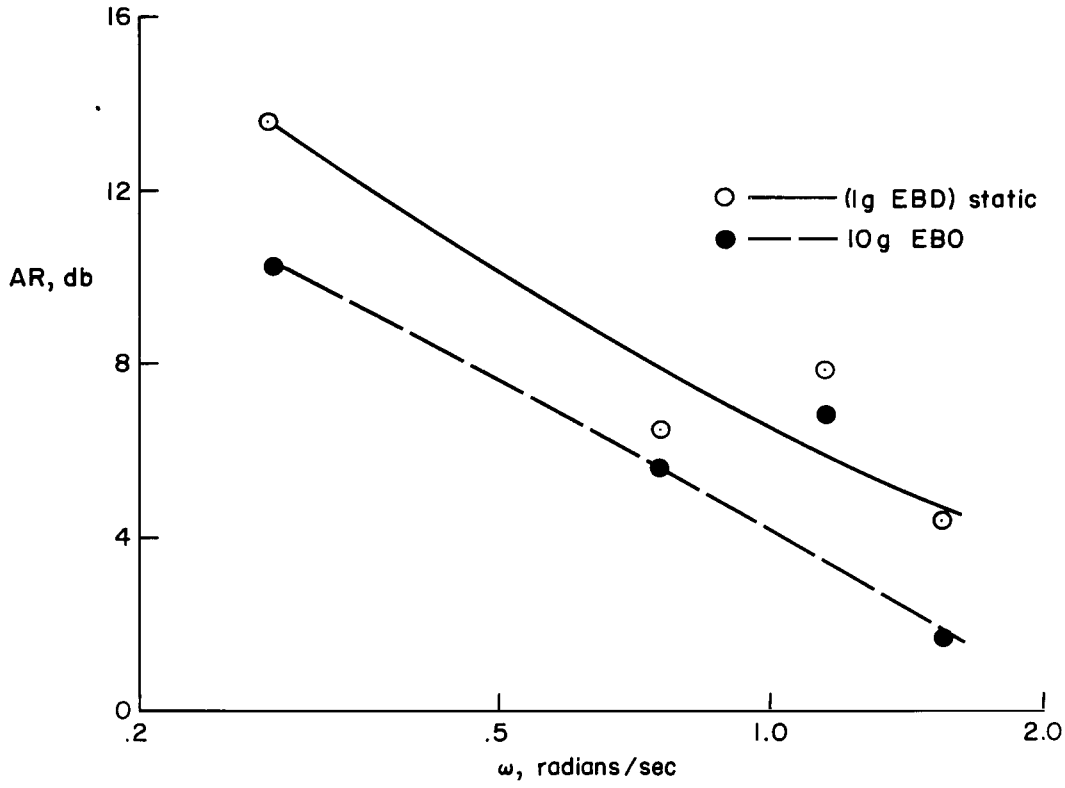

(a) Amplitude ratio, Y_pY_c.

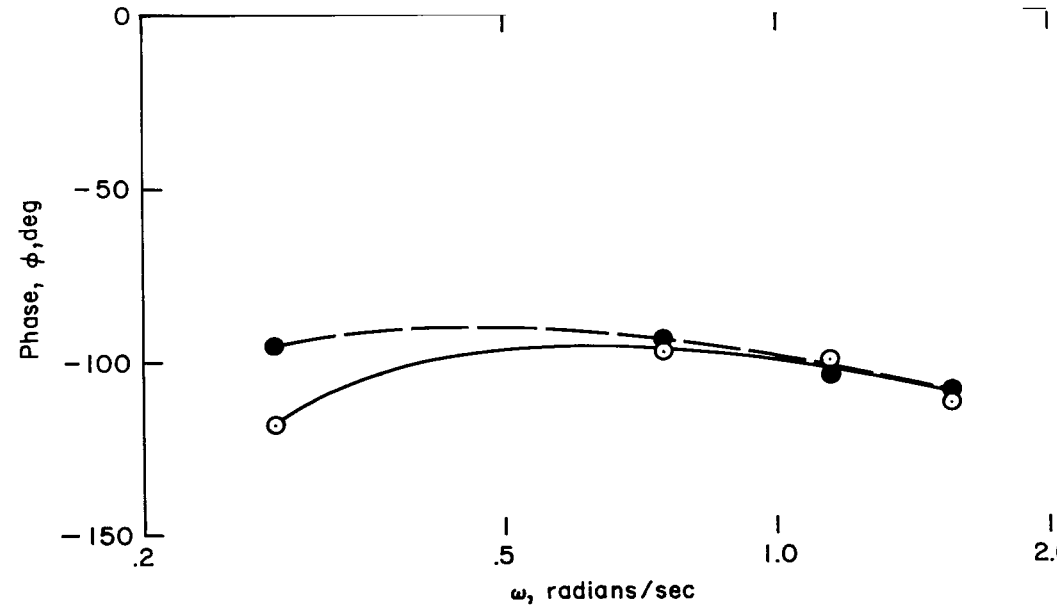

(b) Phase, Y_pY_c.

Figure 18.- Effects of acceleration on open-loop system response (pilot A).

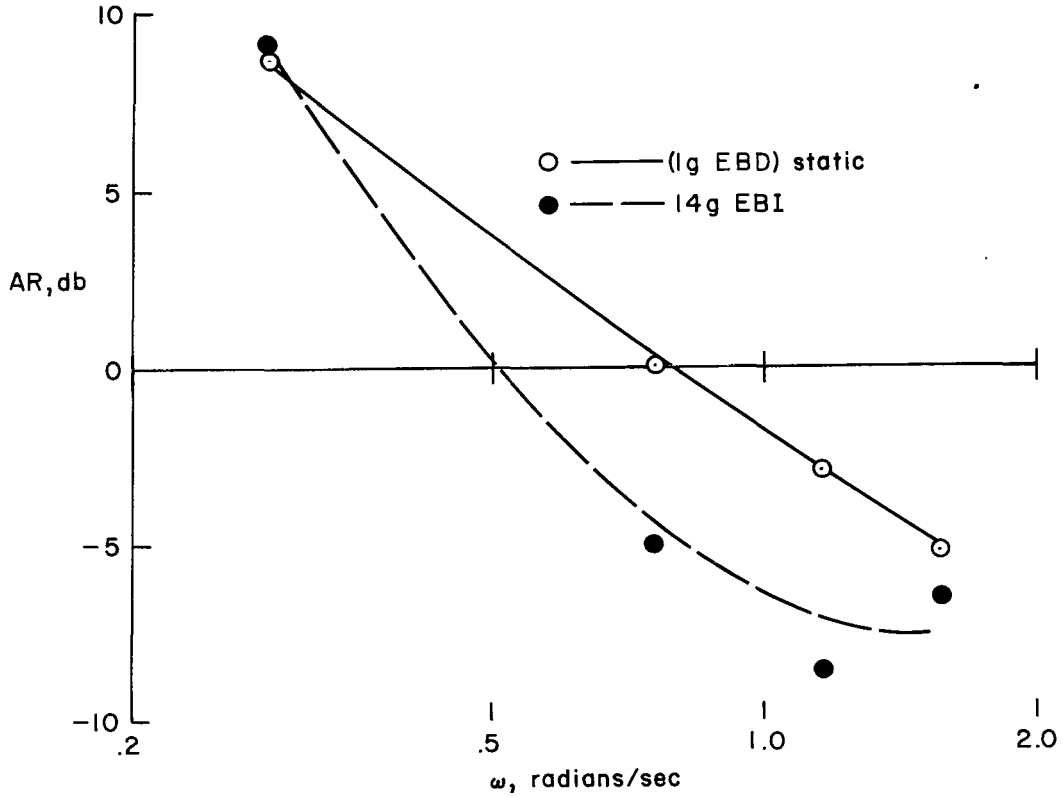

(a) Amplitude ratio

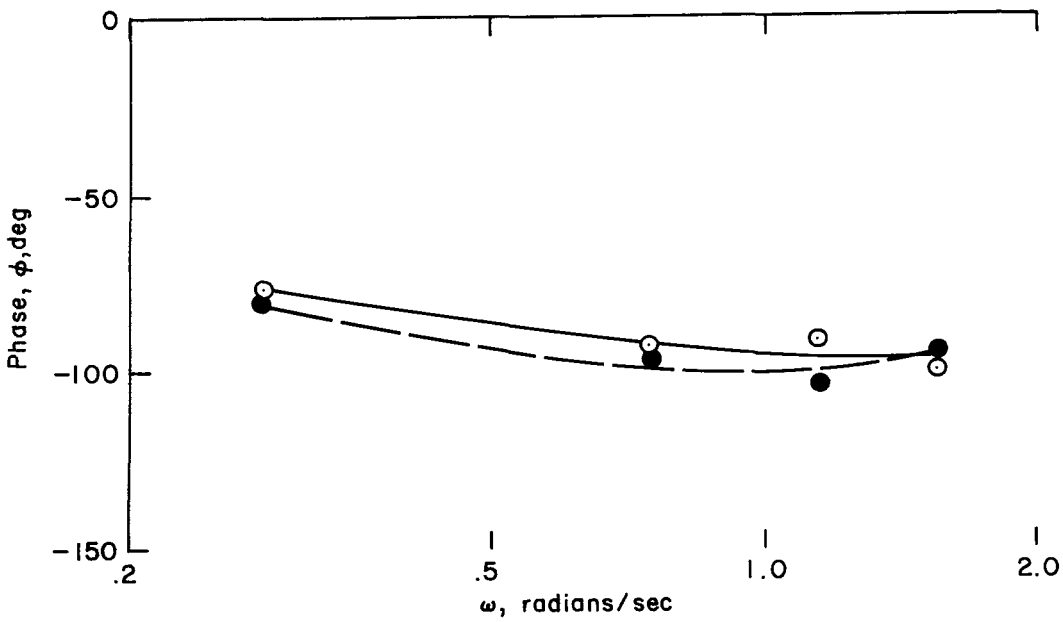

(b) Phase, Y_pY_c.

Figure 19.- Effects of acceleration on open-loop system response (pilot B).

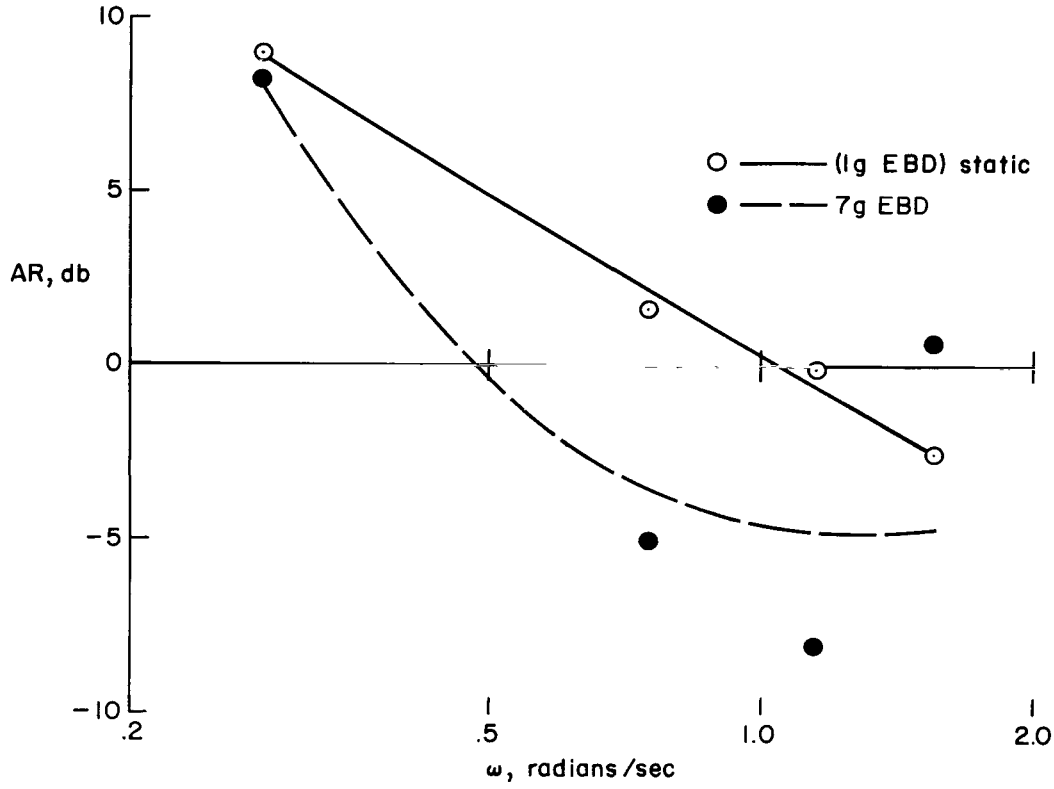

(a) Amplitude ratio, Y_pY_c.

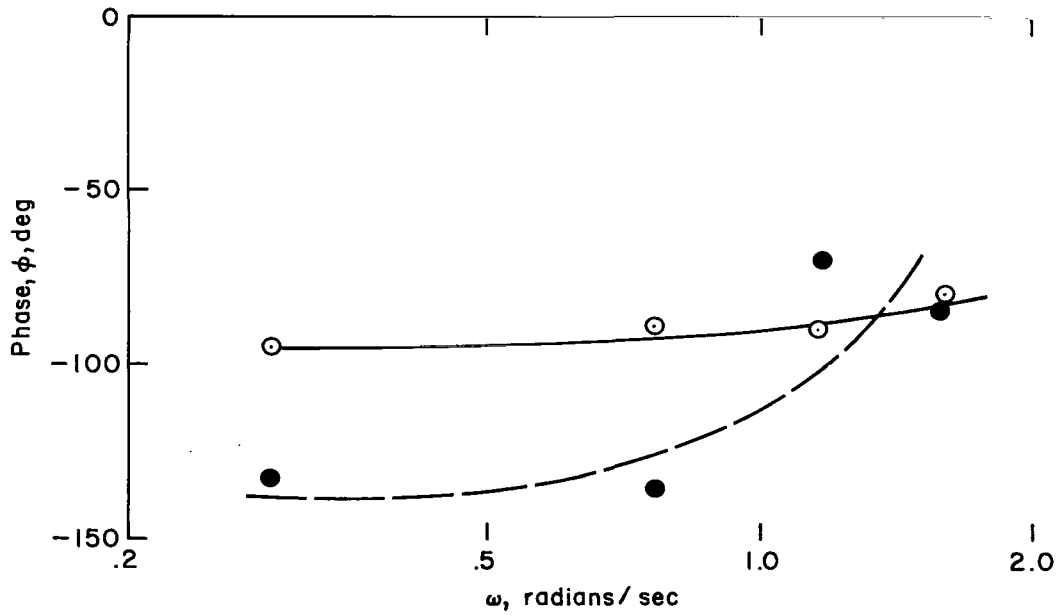

(b) Phase, Y_pY_c.

Figure 20.- Effects of acceleration on open-loop system response (pilot C).

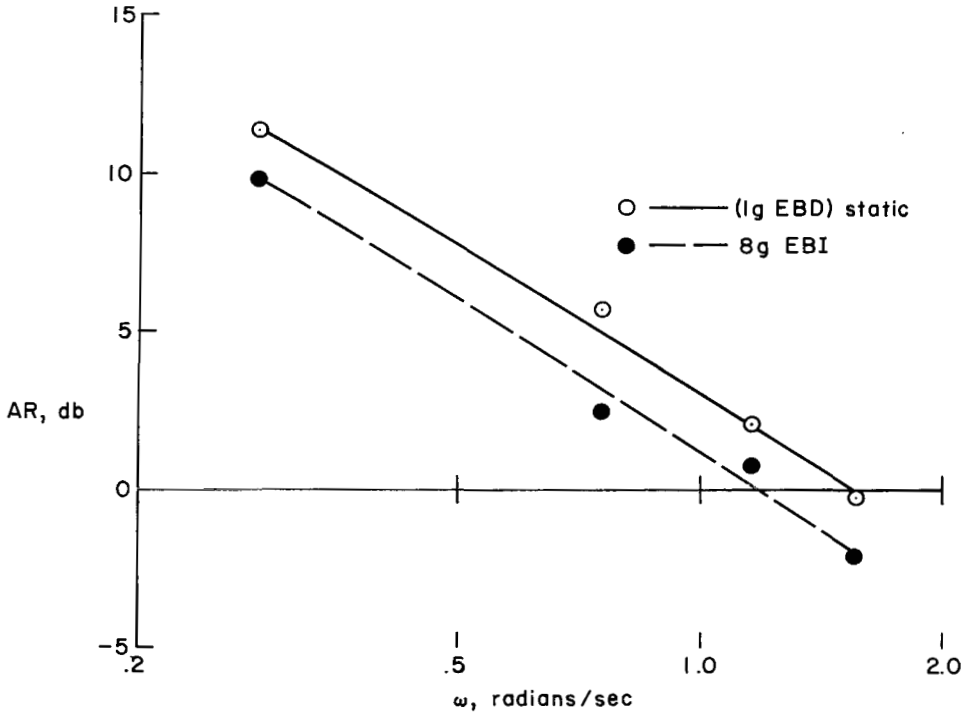

(a) Amplitude ratio, Y_pY_c.

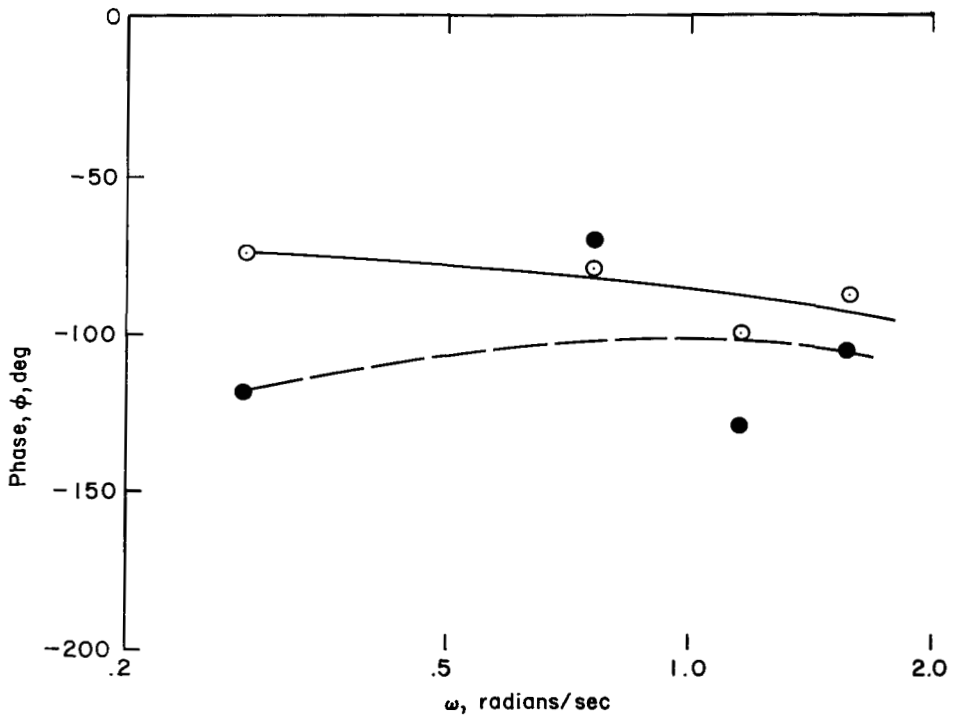

(b) Phase, Y_pY_c.

Figure 21.- Effects of acceleration on open-loop system response (pilot D).

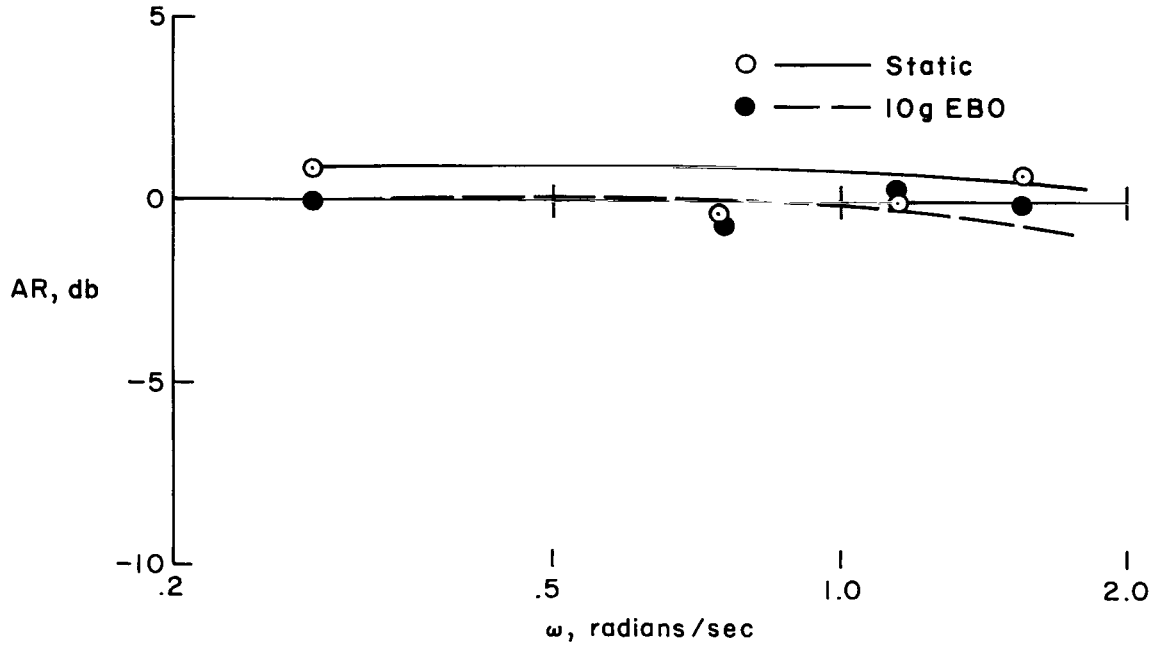

(a) Amplitude ratio, Y_{CL}.

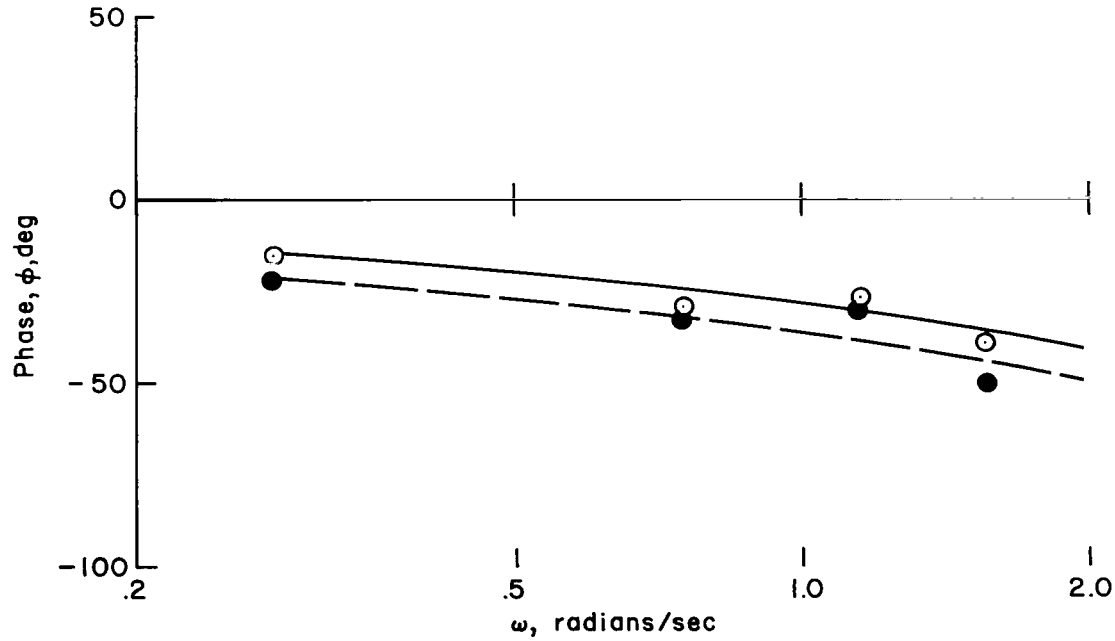

(b) Phase, Y_{CL}.

Figure 22.- Effects of acceleration on closed-loop system response (pilot A).

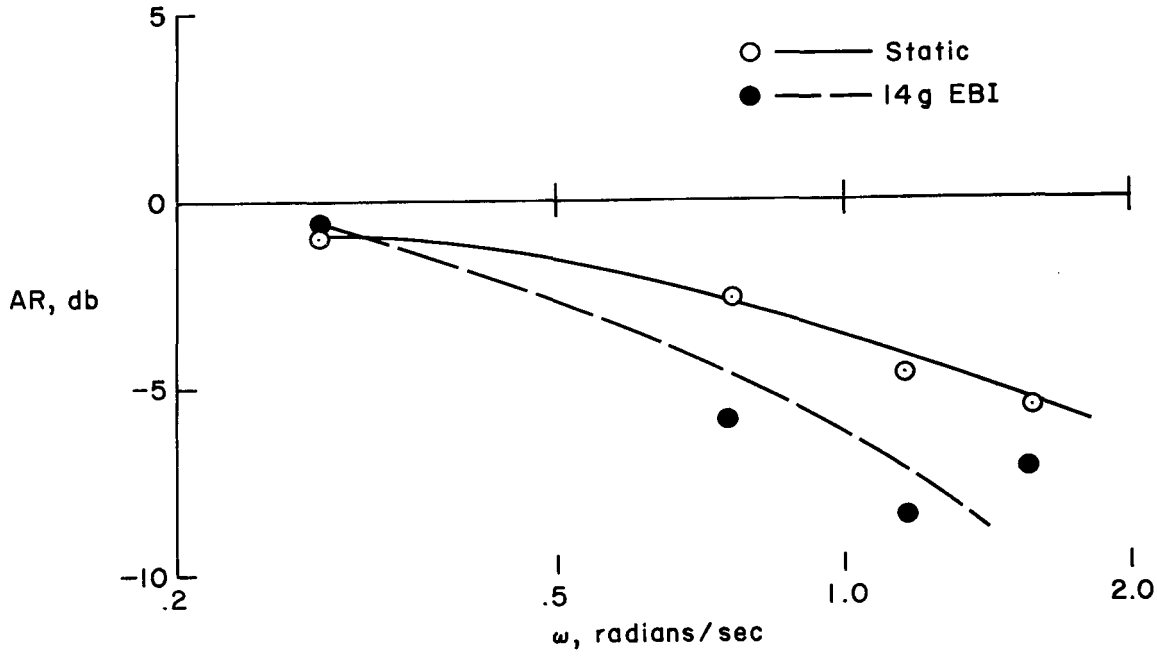

(a) Amplitude ratio, Y_{CL}.

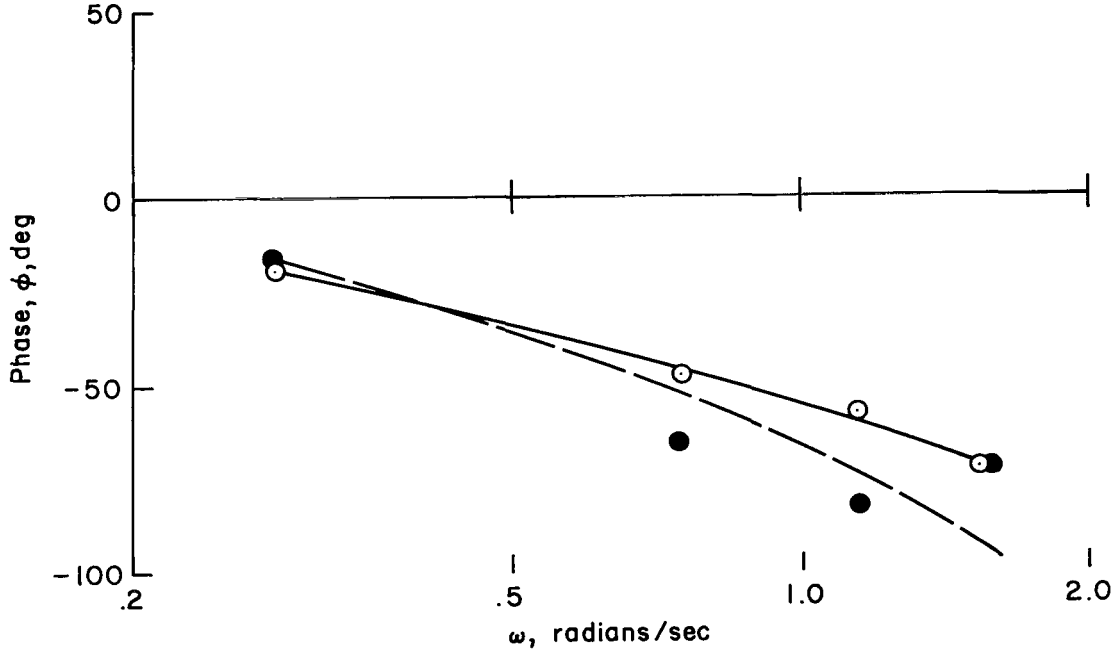

(b) Phase, Y_{CL}.

Figure 23.- Effects of acceleration on closed-loop system response (pilot B).

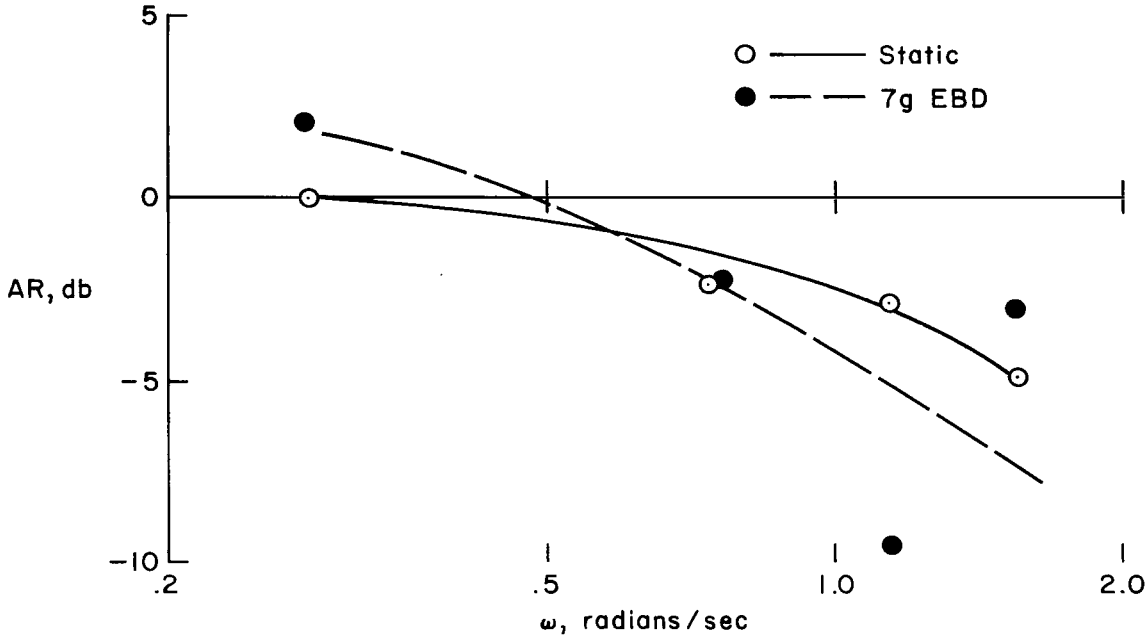

(a) Amplitude ratio, Y_{CL}.

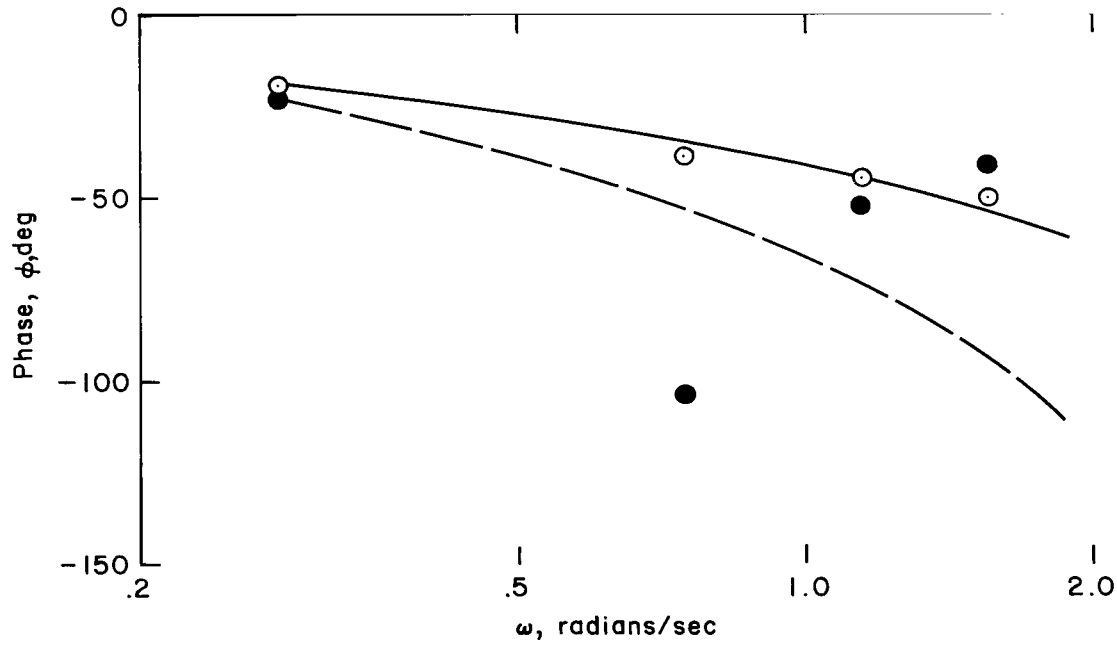

(b) Phase, Y_{CL}.

Figure 24.- Effects of acceleration on closed-loop system response (pilot C).

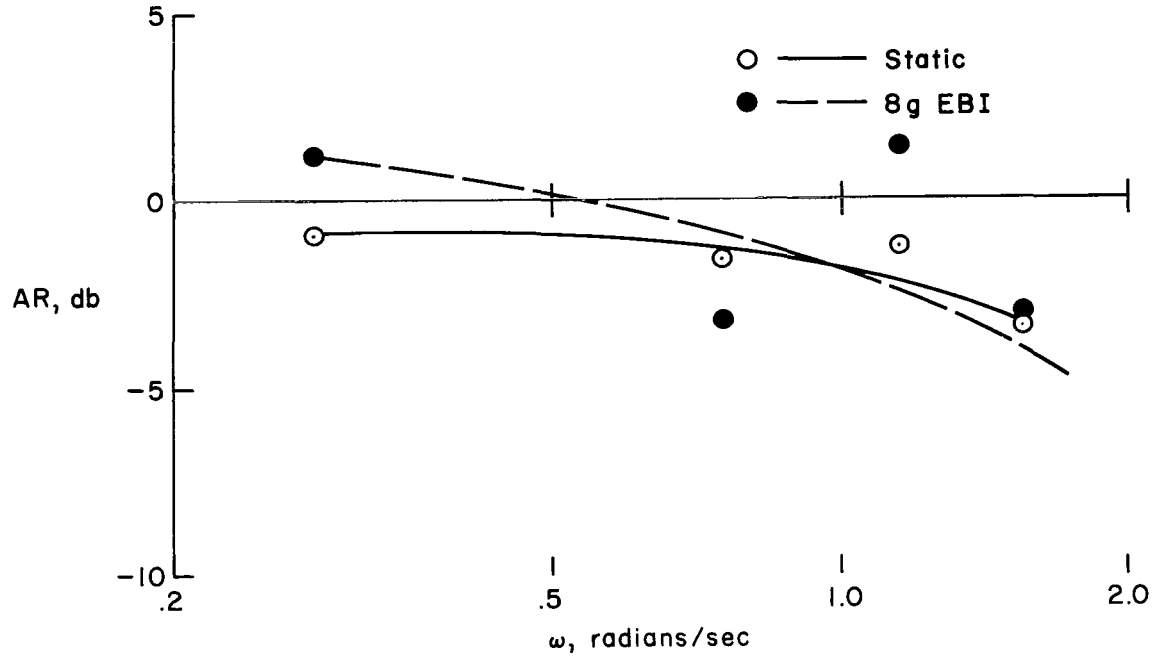

(a) Amplitude ratio, Y_{CL}.

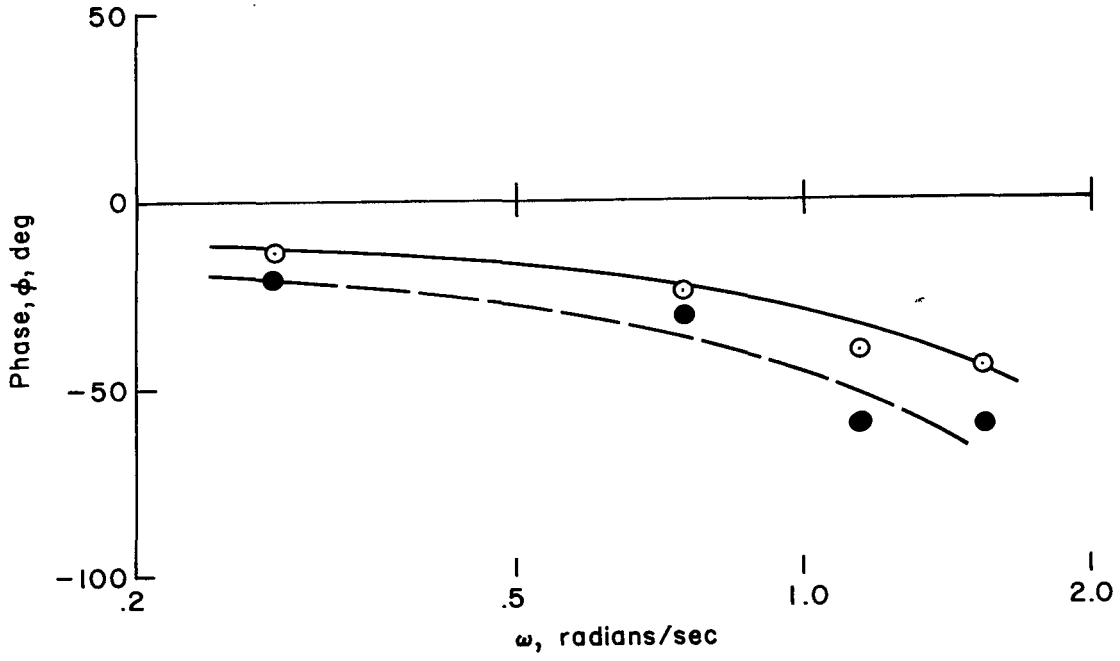

(b) Phase, Y_{CL}.

Figure 25.- Effects of acceleration on closed-loop system response (pilot D).

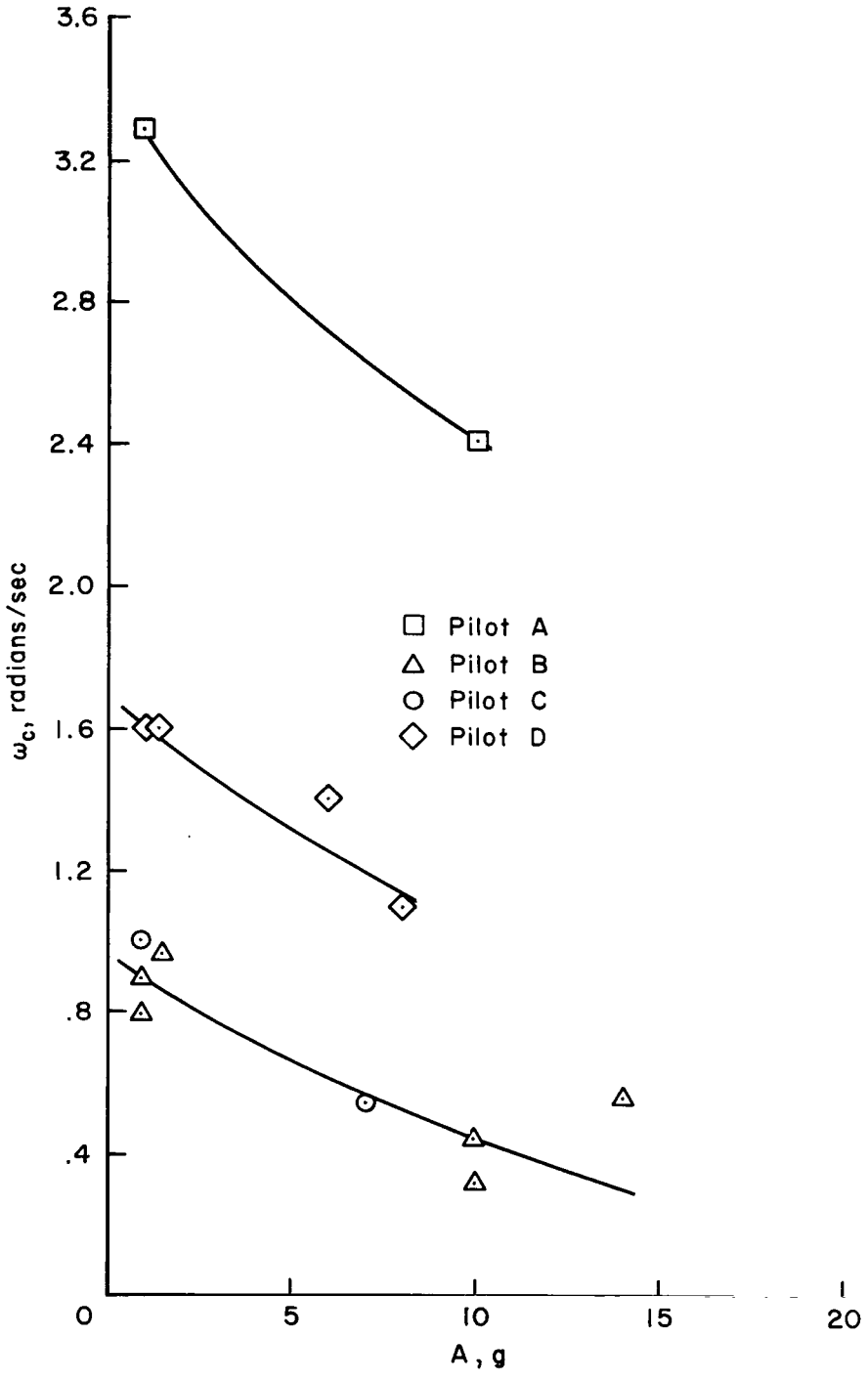

Figure 26.- Effects of acceleration of open-loop crossover frequencies.

+/6125

"The aeronautical and space activities of the United States shall be conducted so as to contribute . . . to the expansion of human knowledge of phenomena in the atmosphere and space. The Administration shall provide for the widest practicable and appropriate dissemination of information concerning its activities and the results thereof."

—NATIONAL AERONAUTICS AND SPACE ACT OF 1958

NASA SCIENTIFIC AND TECHNICAL PUBLICATIONS

TECHNICAL REPORTS: Scientific and technical information considered important, complete, and a lasting contribution to existing knowledge.

TECHNICAL NOTES: Information less broad in scope but nevertheless of importance as a contribution to existing knowledge.

TECHNICAL MEMORANDUMS: Information receiving limited distribution because of preliminary data, security classification, or other reasons.

CONTRACTOR REPORTS: Technical information generated in connection with a NASA contract or grant and released under NASA auspices.

TECHNICAL TRANSLATIONS: Information published in a foreign language considered to merit NASA distribution in English.

TECHNICAL REPRINTS: Information derived from NASA activities and initially published in the form of journal articles.

SPECIAL PUBLICATIONS: Information derived from or of value to NASA activities but not necessarily reporting the results of individual NASA-programmed scientific efforts. Publications include conference proceedings, monographs, data compilations, handbooks, sourcebooks, and special bibliographies.

Details on the availability of these publications may be obtained from:

SCIENTIFIC AND TECHNICAL INFORMATION DIVISION

NATIONAL AERONAUTICS AND SPACE ADMINISTRATION

Washington, D.C. 20546